NUMERICAL INVESTIGATION OF BIOGROUT: A NEW SOIL IMPROVEMENT METHOD BASED ON MICP

A project report

Submitted by

Sumana Bhattacharya

(Roll No. – 213CE1039)

In partial fulfillment of the requirements
for the award of the Degree of

Master of Technology
In
Geotechnical Engineering

Under the guidance of

Dr. Sarat Kumar Das

Department of Civil Engineering
National Institute of Technology, Rourkela, India
May 2015

Department of Civil Engineering
National Institute of Technology, Rourkela
India – 769008,
www.nitrkl.ac.in

CERTIFICATE

This is to certify that the thesis entitled "**Numerical Investigation of Biogrout: A New Soil Improvement Method Based on MICP**" submitted by **Sumana Bhattacharya** bearing roll number 213CE1039, in partial fulfillment of the requirements for the award of the degree of Master of Technology in Civil Engineering with specialization in "Geotechnical Engineering" at National Institute of Technology, Rourkela, is an authentic project work carried out by her under my supervision. The content of this thesis, in full or in parts, has not been submitted to any other Institute or University for the award of any degree or diploma. The sources and aids that are duly mentioned in this work, are the soul resources that have been used.

Place: Rourkela

Date:

Dr. Sarat Kumar Das

Associate Professor

Department of Civil Engineering

National Institute of Technology, Rourkela

India

Acknowledgements

I would like to express my sincere gratitude towards my project advisor **Dr. Sarat Kumar Das** for his consistent guidance, invaluable suggestions and encouragement throughout the entire work and in preparation of this thesis. His inspiring words and kind support have always motivated me to work hard and finish my work in a timely manner. I am truly grateful to him for believing in me and providing unconditional support throughout the tenure of the work.

I would also like to thank **Dr. Suresh Prasad Singh** for setting an example of a dedicated and hard-working person in front of me. His commitment towards his work and amicable nature has inspired me throughout the project.

Finally, thanks to **NIT Rourkela** for giving me this auspicious opportunity to carry out this project.

Sumana Bhattacharya

NIT Rourkela

Roll No. : 213CE1039

Abstract

Ground improvement is essential in regions where the desired mechanical properties of soil are not suitable for the particular use. Microbial induced calcite precipitation (MICP) offers an alternative solution to a wide range of civil engineering problems. The microbial urease catalyzes the hydrolysis of urea into ammonium and carbonate. The produced carbonate ions precipitate in the presence of calcium ions as calcium carbonate crystals. Recently, MICP has also been shown to improve the undrained shear strength, confined compressive strength, stiffness and liquefaction resistance of soils and offers potential benefits over current ground improvement techniques. Biogrout is the new ground improvement method where MICP is used to achieve soil strength and stiffness. There is a need to clearly understand the various bio-geo-chemical processes that take place during biogrout in order to predict the enhancement in different mechanical properties of soil.

The aim of this master's thesis is to present a numerical model for biogrout process for one-dimensional column experiment, investigating the influence of different injection schemes on the distribution of precipitated calcite within the porous media. In this work, a multi-component bio-geo-chemical model was used, based on the coupled code OpenGeoSys-PhreeqC. The applied model describes the physical and chemical process during the different injections. The results show that the reduction of porosity and permeability can be manipulated using different injection schemes.

Contents

List of Figures

List of Tables

Chapter 1

Introduction

1.1 Motivation

In many parts of the world the mechanical properties of soils are insufficient to sustain the designed structural load. Stability of slopes becomes a serious issue as they become unstable over time. Roads and railways undergo significant settlement and require continuous maintenance. Liquefaction as a result of earthquake in earthquake-prone areas causes loss of life and damage to properties. Land erosion by running water in coastal or alluvial regions gives uncertainty to the structural life in those areas. Formation of sinkholes due to gradual or sudden removal of soluble bedrock, collapse of cave roof or lowering of water table poses threat to structures constructed on top of them.

Ground improvements in these areas are essential before and after construction. Modern geo-engineering provides a host of different methods for in-situ soil stabilization and ground improvement. Ground improvement techniques such as stone columns, soil nails, micropiles, jet grouting, ground anchors, geosynthetics and surface compaction provide sufficient strength for low strength soil and are in use for many years as conventional ground reinforcement techniques. Other techniques such as lime and cement stabilization and freezing are also extensively used in certain regions under certain circumstances especially for underground constructions.

Traditional ground improvement methods have certain limitations and disadvantages. The action radius is limited to the proximity of the mixing equipment. High pressures are often required to inject the grouts due to their high viscosity or fast hardening time. Freezing is only a temporal solution during construction. Moreover most of these methods are expensive, require heavy machinery, disturbing urban infrastructure and involve chemicals with significant environmental impact. Finally, these methods significantly reduce the permeability of the strengthened soil, which hinders groundwater flow and limits long distance injection. Consequently, these conventional methods are not suitable for treating large volumes of soil (van Paassen, 2009).

Calcite precipitation can occur naturally when there is an excess of calcium ions in a solution. However, bacterial strains producing urease can have a considerable impact on the precipitation process if they are supplied with calcium and urea. By temporarily regulating the concentration of bacteria and nutrients in a soil, a new engineering material can be generated through bacterially induced calcite cementation of the existent soil matrix. This approach can be used to decrease the permeability and the compressibility of the soil and increase the strength of the soil (van Paassen, 2009).

Biogrout is an in-situ soil strengthening technique involving microbial induced carbonate precipitation (MICP). This process involves hydrolysis of urea by bacteria containing the enzyme urease in the presence of dissolved calcium ions, resulting in calcium carbonate precipitation.

In order to control the Biogrout process for engineering applications, it is necessary to improve understanding of the relevant phenomena and develop efficiencies to enable up-scaling of the technology to suit commercial applications (van Paassen, 2009).

Understanding, controlling and predicting this alternative environmentally friendly soil reinforcement technique enables many geo-engineering problems to be reconsidered and exposes innovative applications, such as restoration of weak foundations, seismic retrofitting, erosion protection and maintenance of railway tracks. MICP has been experimentally investigated during the past decade by several researchers (van Paassen, 2009; Dejong et al. 2006; Whiffin et al. 2007), yielding a reasonable level of understanding of the involved processes. However, the prediction of MICP is still relatively unexplored, with the exception of the recently published developments by Martinez et al. (2011), van Wijngaarden et al. (2011) and Fauriel and Laloui (2012). Thus, there is a clear need to further develop comprehensive bio-geo-chemical mathematical modelling capacities that are able to realistically predict the multispecies reactive transport in saturated, deformable soils (Fauriel and Laloui, 2012).

The aim of this master's thesis is to investigate the influence of different injection schemes with different durations and concentrations of injected components the on calcite precipitation during MICP simulation on a spatial scale which is relevant for one-dimensional column experiment.

1.2 Objective and Scope

The objective of this study is to develop a general numerical model to describe the injection, the distribution and the reaction processes of biogrout within a saturated, deformable porous medium.

The objectives can be classified as

- Prediction of spatial and temporal distribution of calcite precipitation at continuum scale to provide insights to laboratory and field applications.
- The coupled various geochemical processes can be better understood by sequential implementation in the simulations
- Understanding how solutes move in subsurface systems and how it reacts with surrounding geological environment
- Measurement of the change in porosity/permeability in order to have an idea about soil strength gain

In this study, a numerical model has been developed to investigate various coupled bio-geo-chemical processes that occur during the biogrout process. OpenGeoSys and PhreeqC has been used to perform the simulation. Urea hydrolysis and calcite precipitation has been modeled as kinetic equations in PhreeqC. A one-dimensional domain has been considered for the analysis. The results show calcium carbonate precipitation and concentration distribution throughout the entire domain. It also shows variation of porosity and permeability as a result of mineral calcite precipitation, throughout the domain.

1.3 Structure of the Independent Study

This master's thesis consists of 6 chapters: introduction, literature review, fundamentals, concept of the developed model, results and summary. The introduction gives a short description of the problem, motivation to carry out research in this area and objective of the present study. Chapter 2 presents the fundamentals of MICP technology and fundamentals of biogrout process. It also presents fundamentals of groundwater flow and mass transport through porous media and fundamentals of geochemical modeling. Chapter 3 gives the detailed literature review. Chapter 4 deals with the model concept. Section 4.1 gives the main assumptions of the model. Brief description of coupled code OpenGeoSys-PhreeqC is given in Section 4.2. Different injection schemes are described in Section 4.3. The subsequent sections discuss about various model parameters, kinetics, governing equation for porosity and permeability update, etc. Results of the simulations are given in Chapter 4. Section 5.1 deals with the model domain and Section 5.2 provides the results obtained for 2-phase scheme implementation. Section 5.3 gives results obtained for 1-phase scheme implementation. Section 5.4 gives the comparison of the two mechanism. Chapter 6 gives the summary of the obtained results and recommendations for the future extension to obtain a more accurate model.

Chapter 2

Fundamentals

2.1 Introduction to MICP

2.1.1 MICP

Bacteria are the dominant microorganisms in soils. When supplied with suitable substrates, bacteria can catalyze chemical reactions in the subsurface resulting in precipitation (or dissolution) of inorganic minerals, which change the mechanical soil properties.

Most of the inorganic carbon on the earth surface is present as layers of limestone of which a significant portion is of biogenic origin. Many bacteria can induce the precipitation of calcium carbonate, but not all can be used for ground improvement. Sporosarcina pasteurii is a common soil bacterium naturally occurring in the subsurface. It uses urease to increase pH and thereby to kill other bacteria to get rid of competitors. S. pasteurii is an aerobic bacterium, which use oxygen for the oxidation of the substrate. Precipitation of calcium carbonate occurs when a solution is oversaturated, the amount of calcium and carbonate ions in solution exceeds the

solubility product, i.e. the solution gets oversaturated. The role of bacteria in calcium carbonate precipitation is attributed to (van Paassen, 2009):

1. Producing carbonate (e.g. by hydrolysis, respiration, etc.).

2. Producing alkalinity (increasing the pH locally, which causes the dissolved inorganic carbon which is mainly present as bicarbonate to dissociate causing an increase in carbonate concentration).

3. Acting as nucleation sites in an already oversaturated solution.

All bacteria cells require a constant supply of energy to survive. Bacteria use substrate as a source of energy. Depending on the species of bacteria different substances may be used as substrate.

To stimulate microbially induced calcium carbonate precipitation in the subsurface, micro-organisms or substrates have to be injected and transported over a substantial distance into the porous material. Transport of bacteria (and hence bacterial activity) is limited in fine grained soils. As bacteria have a typical size of 0.5 to 5 μm, they cannot be transported through silty or clayey soils, nor can their activity be used to induce carbonate precipitation in these layers (Mitchell & Santamarina, 2005).

2.1.2 MICP by Urea Hydrolysis

In natural environments, the primary means by which microorganisms promote calcium carbonate precipitation is by metabolic processes that increase the alkalinity of the soil. In MICP, by way of urea hydrolysis, bacteria processing the enzyme urease can use urea $\left(\left(NH_2\right)_2 CO\right)$ as an energy source and produce ammonium $\left(NH_4^+\right)$. More specifically, the hydrolysis of urea is catalyzed by urease, producing ammonium and carbonate ions CO_3^{2-} according to Eq. (2.1). Ammonium then dissociates to ammonia NH_3 as a result of the pH increase, until equilibrium between NH_4^+ / NH_3 and HCO_3^- / CO_3^{2-} is reached at a pH of approximately 9.3. The hydrolysis of urea is a homogeneous reaction that takes place within the fluid phase, causing mass transfer among the components of the fluid phase.

$$CO\left(NH_2\right)_2\left(aq\right)+2H_2O\left(l\right)\xrightarrow{urease}2NH_4^+\left(aq\right)+CO_3^{2-}\left(aq\right) \tag{2.1}$$

Upon hydrolysis of urea, the products of Eq. (2.1) further react into a wide range of dissolved species, including carbonate, bicarbonate $\left(HCO_3^-\right)$, carbonic acid $\left(H_2CO_3\right)$, hydroxide $\left(OH^-\right)$ and protons $\left(H^+\right)$. In the presence of calcium ions $\left(Ca^{2+}\right)$, dissolved complexes can form with the anions (e.g., calcium carbonate $\left(CaCO_3\right)$). This speciation is governed by acid–base equilibria and depends on pH, temperature and salinity.

Finally, the last reaction type involved in MICP is mineralization. The mineralization itself consists of several phases characterized by different rates: nucleation, crystal growth and

secondary changes in the crystal lattice. If a sufficient amount of carbonate is produced, then the solution becomes oversaturated, and calcium carbonate can precipitate (Eq. (2.2)). Eq. (2.2) corresponds to a heterogeneous precipitation reaction, which adds mass to the matrix.

$$Ca^{2+} + CO_3^{2-} \rightarrow CaCO_3(s) \tag{2.2}$$

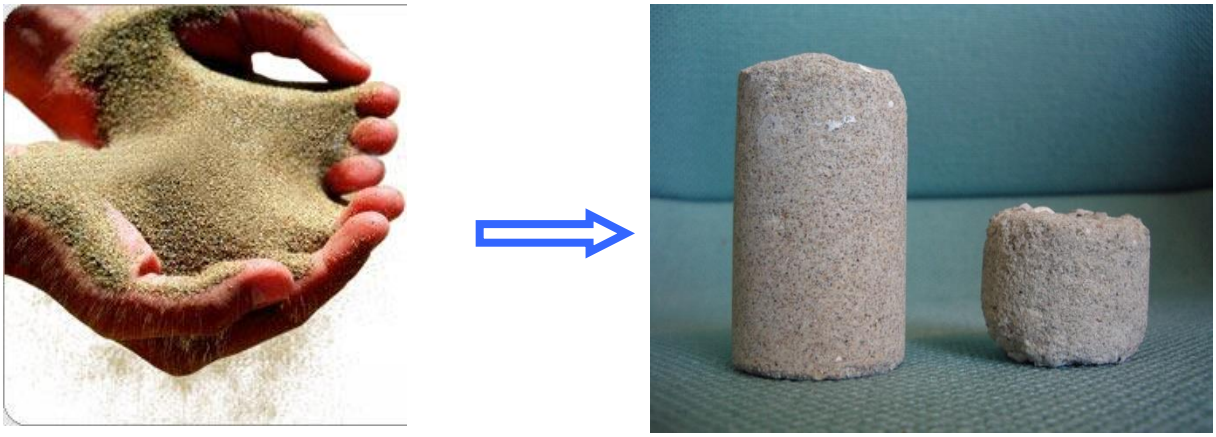

Fig. 2.1: Conversion of sand to sandstone by MICP

(Photo:http://www.ciflorestas.com.br/conteudo.php?id=9344)

2.1.3 Civil Engineering Applications of MICP (Parks, 2009)

The use of these bacteria in biotechnological applications is appealing for many reasons. One is that urease, the enzyme that catalyzes the hydrolysis of urea to ammonia and carbon dioxide, is common in a wide variety of soil and aquatic bacteria (Warren et al., 2001), and so the introduction or use of foreign bacteria may not be required. Another is that urea, an important nitrogen compound found in natural environments, is a fairly inexpensive substrate (Hammes et al., 2003a). Also, the use of bacteria to raise the pH in the environment is preferable to the direct injection of a base because the gradual hydrolysis of urea is likely to promote a wider spatial

distribution of calcite, whereas the direct addition of base is likely to cause immediate precipitation at the injection site (Ferris et al., 2003).

1. Structural Engineering:

Bacteriogenic Mineral Plugging: An innovative use for calcite precipitation by ureolytic bacteria is the plugging of cracks and preferential pathways in porous media. This technique controls subsurface fluid movement through the reduction of porosity and permeability of both geologic formations (Ferris et al., 1996) and manmade structures like concrete and cement (Ramachandran et al., 2001).

Bio-Brick (biomason.com): The built environment is currently constructed using a limited palette of traditional materials: concrete, glass, steel and wood. Traditional materials contain a high-embodied energy, and rely heavily on limited natural resources. The manufacture of concrete, one of the most energy intensive materials, uses limestone shale converted into Portland cement through high-heat processes. Global cement production in 2008 amounted 2.8 billion tons, with equivalent quantities of CO_2 released into the atmosphere. Both concrete and clay manufacturing include energy intensive processes for raw material extraction, transportation, and fuel sources for heating kilns. 40% of global carbon dioxide emissions are linked to the construction industry, primarily owing to exhaustive material production and disposal processes. At bioMASON.inc, materials are grown by employing microorganisms to grow cement. The process of growing bricks is similar to hydroponics- whereby units mixed with the microorganism are fed an aqueous solution to harden the bricks to specification. Traditional bricks are formed in brick units and then fired for hardening. bioMASON's process

eliminates the need for firing by replacing the curing/hardening process with the formation of biologically controlled structural cement.

2. Environmental Engineering:

Environmental Remediation of Radionuclides: Department of Energy (DOE) operations in the western U.S. have left groundwater contaminated with divalent metals (Pb, Zn, Cd), and radionuclides ($^{99}Sr, UO_2^{2+}$ *and* ^{60}Co) (Riley and Zachara, 1992). It is possible that some of these elements can be incorporated into calcite crystals either by substituting for calcium or by occupying vacancies in the crystal lattice (Veizer, 1990). Strontium can readily substitute for calcium. There is evidence that the fine-grained carbonate minerals formed by microbial activity may incorporate more strontium than crystals formed abiotically (Ferris et al., 1995). Bacterial ureolysis is a particularly good application in this situation because the large volume of contaminated material deep in the subsurface calls for a cost effective, *in situ* method for containment and stabilization (Fujita et al., 2000, 2004; Mitchell and Ferris, 2005). Higher ureolysis and precipitation rates have been shown to allow for more Strontium to be incorporated into the carbonate minerals (Fujita et al., 2004; Mitchell and Ferris, 2005). Also, as opposed to abiotic injection of reagents, the bacterially induced precipitation can achieve a wider spatial distribution in the aquifers, allowing radionuclides to be precipitated over a larger area.

3. Geotechnical Engineering:

Soil Improvement: Improvement of soil strength is possible using ureolytic bacteria. Reduced permeability has been shown to occur when a mixture of bacteria and reagents are either sprayed

on the soil, or injected into the soil at high velocity and pressure (Whiffin et al., 2007). Whiffin et al. (2007) determined that soil strengthening can be achieved and permeability maintained when the bacteria and reagents are injected at low velocities, and the urea hydrolysis rate is balanced with the reactant flow rate to achieve soil strengthening in the desired locations.

4. Energy Geotechniques and Sustainability:

Enhanced Oil Recovery: Heavy crude oil, found in Canada, Alaska, Venezuela and other areas, is highly viscous and does not flow well. Because water responds better to pumping than heavy oil, only a portion of the oil contained in some reservoirs can be recovered. To increase the yield of oil, enhanced oil recovery techniques are used. The most common of these is the injection of gas (carbon dioxide, natural gas, and nitrogen are frequently used), which expands and thereby pushes oil into the well. The injected gas can also diffuse into the oil, thereby lowering its viscosity and making it easier to pump. Alternatively, selectively plugging high permeability areas in the reservoirs may be a way to control excess water production. Ferris et al. (1996) explored the possible use of ureolytic bacteria to precipitate calcium minerals in high permeability water channels. In their studies, indigenous bacteria were grown in sand cores, after which the permeability of the cores was tested. They found a significant reduction in permeability, suggesting that this is a very feasible method for enhanced oil recovery.

Carbon Sequestration: Geologic carbon sequestration involves capturing carbon dioxide (CO_2) from point sources like power plants, and storing it underground in deep saline aquifers instead of allowing its release into the atmosphere. Not much is known about how the CO_2, which will be in a supercritical phase ($scCO_2$) at the pressure and temperatures found in these aquifers, will

behave. Zero Emissions Research and Technology (ZERT), a DOE funded project, is developing technologies to monitor and map the movement of CO_2 once it has been injected. There is concern that the CO_2 could migrate back to the Earth's surface via preferential pathways like old well bore holes and cracks in the cap rock. Bacteriogenic mineral plugging can potentially be used to seal these pathways, and keep the CO_2 underground. The $scCO_2$ may also be permanently sequestered if it can be converted into carbonate minerals such as $CaCO_3$.

2.2 Introduction to Biogrout

The mechanical properties of soil (cohesion, friction, stiffness, permeability) are important when engineering constructions in sedimentary environments. Traditionally, soil properties are specific for each location depending on current and historical sedimentary conditions and on human interventions. When soils are unfavorable for desired use measures can be taken. For example, the stability of slopes can be improved using anchors, bolts and fences, but also vegetation can have a positive effect on slope stability (Fan and Su 2008; Normaniza et al. 2008). Erosion and deposition of soils along coasts and river banks can be controlled by continuous dredging and nourishment, by introducing constructions like dikes, jetties, groins and breakwaters, by making use of reefs (Frihy et al. 2004) and vegetation or by integrated approaches (Jones and Hanna 2004).

Recently, techniques are being developed, which aim at changing soil properties on demand by stimulating natural (bio-)chemical processes in situ (Whiffin et al. 2005; Van Meurs et al. 2006; Ivanov and Chu 2008). One of these technologies is Biogrout: an in situ soil strengthening technique, involving microbial induced carbonate precipitation (van Paassen, 2009).

In order to induce MICP in the soil subsurface, reagents and catalysts need to be injected and transported to the location where strengthening is required. Treatment over large distances is preferred for economical reasons (to limit the number of required injection wells) and enable ground improvement without disturbing the serviceability of any urban infrastructure present in the vicinity (van Paassen, 2009). Mixing bacteria and reagents prior to injection results in immediate flocculation of bacteria and crystal growth. Whilst this method can be applied for treatment of surfaces, very coarse grained materials and mixed in place applications, this would cause rapid clogging of the injection well and surrounding pore space for many (fine) sands. In order to prevent crystal accumulation around the injection point and encourage a more homogeneous distribution of $CaCO_3$ over large distance, a two-phase injection for bacterial retainment has been suggested (Whiffin et al. 2007).

Biogrout procedure would involve the following steps (van Paassen, 2009):

1. Cultivate suitable micro-organisms in the laboratory (or in the subsurface).

2. Inject micro-organisms (and nutrients) in the ground and transport them to the desired location.

3. Supply the micro-organisms with suitable substrates to induce a biochemical conversion resulting in precipitation of calcium carbonate.

4. Remove the remaining products.

5. In order to use Biogrout for engineering applications it is important to precipitate calcium carbonate homogeneously throughout the entire treated sand body, preferably over large injection distance, within short time and using as little flushed volume as possible. To achieve homogeneous strength it is considered essential to control the transport and adhesion of bacteria, or better their urease activity, which defines the precipitation rate and hence the distribution of $CaCO_3$ crystals both spatially and temporally (van Paassen, 2009).

Whiffin et al. (2007) showed that low calcium carbonate concentrations (below 60 mg/cm^3) did not significantly improve the strength of the samples. At higher calcium carbonate contents there was a significant improvement in strength relative to untreated sand. The highest strength in the column under experiment was 570 kPa, which was measured at the same location as the maximum amount of $CaCO_3$, at approximately 1 m from the injection point. An apparent minimum calcium carbonate content of 60 kg/m^3 was required for a measurable strength improvement in the material under the testing conditions.

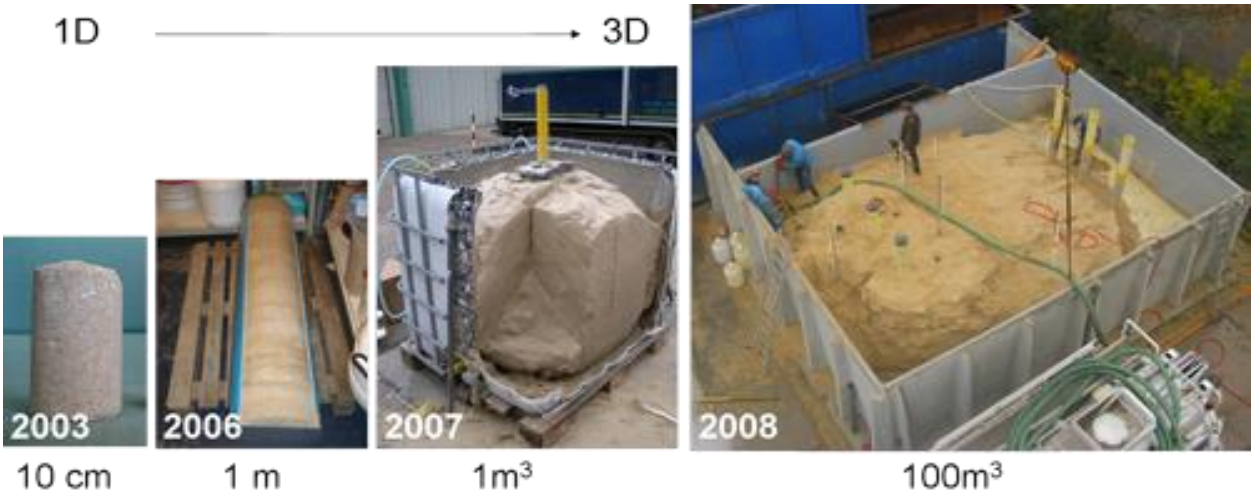

Fig. 2.2: Biogrout experiments (Photo: Deltares)

2.3 Flow and mass transport through porous media

2.3.1 Equations for ground water flow

Darcy's Law: In the mid-1800s, French Engineer Henry Darcy, studied the movement of water through a porous medium. He found out that if h_A and h_B are the hydraulic head (m) at the inlet and outlet of a sand column with length L (m), the flow $Q\left(m^3 s^{-1}\right)$ is proportional to the cross-sectional area of the pipe $A\left(m^2\right)$. When combined with the proportionality constant, $K\left(m\,s^{-1}\right)$, the result is the expression known as Darcy's Law:

$$Q = -KA\left(\frac{h_A - h_B}{L}\right) \tag{2.3}$$

This may also be expressed in a general form as

$$Q = -KA\left(\frac{dh}{dl}\right) \tag{2.4}$$

where $\frac{dh}{dl}$ is known as the hydraulic gradient. The quantity dh represents the change in hydraulic head between two points that are very close to each other and dl is the small distance between these points. The negative sign indicates that the flow is in the direction of decreasing hydraulic head. If the flow rate $q\left(m\,s^{-1}\right)$ is expressed in per unit cross section,

$$q = \left(\frac{Q}{A}\right) = -K\left(\frac{dh}{dl}\right) \tag{2.5}$$

Representative Elementary Volume (REV): For modeling of groundwater flow, it is not possible to catch all the microscopic structure of the porous media. To understand and formulate the dynamics of fluid in the subsurface, the representative elementary volume (REV) is introduced. Parameters are averaged over such a volume that is sufficiently large to describe the porous media at macroscopic scale (Fig. 2.3). Within the REV the detailed structure of the medium is lost and becomes a continuous field. Parameters like porosity, permeability and dispersivity areconsidered constant over the averaging volume. In the following sections material parameters and governing equations are based on the continuum approach.

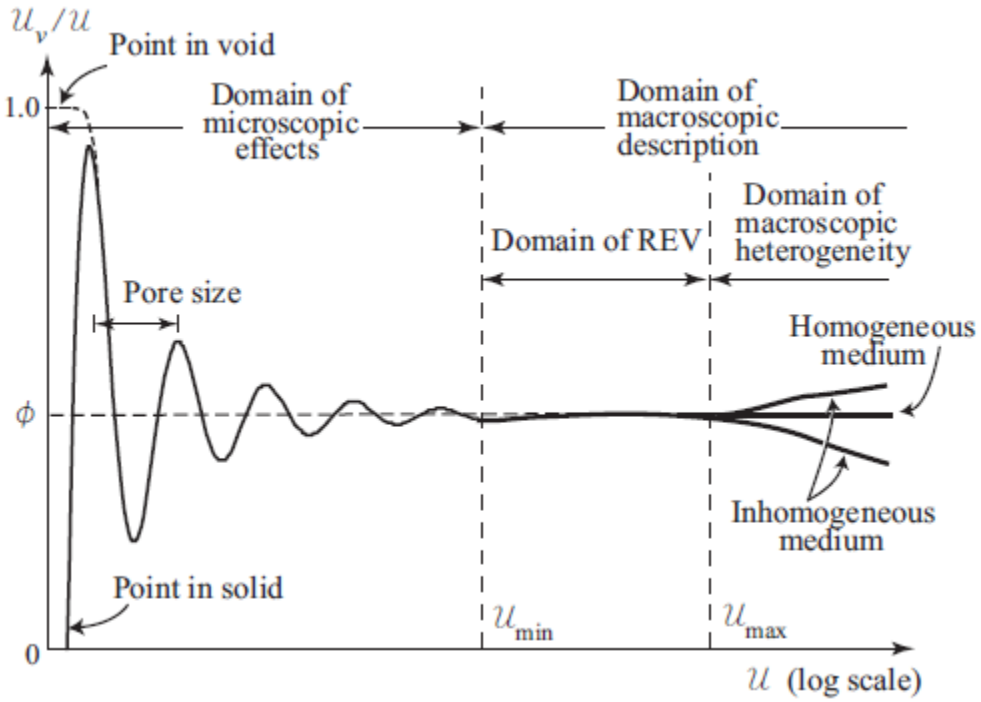

Fig. 2.3: Representative elementary volume concept (Bear, 1972)

Confined Aquifer: The governing equation for flow in confined aquifer is derived from two basic laws of physics, which is the law of mass conservation and the law of energy conservation.

The former states that there can be no net change in the mass of a fluid contained in a small volume of an aquifer, the later states that the amount of energy is a constant within any closed system. Assuming a very small piece of confined aquifer, called a controlled volume, the three sides are of the length *dx*, *dy* and *dz*, respectively. The area of the faces normal to the *x*-axis is *dydz*; the area of the faces normal to the *z*-axis is *dxdy*. If the aquifer is homogeneous and isotropic, the fluid moves in only one direction through the controlled volume, then the actual fluid motion can be subdivided on the basis of the components of flow parallel to the three principle axes. If *q*is flow per unit cross-sectional area, $\rho_w q_x$ is the portion parallel to the *x*-axis, where ρ_w is the density of water. The mass flux into controlled volume is $\rho_w q_x dydz$ along *x*-axis. The mass flux out of the controlled volume is $\rho_w q_x dydz + \frac{\partial}{\partial x}\left(\rho_w q_x\right) dxdydz$. The net accumulation in the controlled volume due to movement parallel to the *x*-axis is equal to the inflow less than the outflow, or $-\frac{\partial}{\partial x}\left(\rho_w q_x\right) dxdydz$. Since there are flow components along all three axes, similar terms can be determined for the other two directions: $-\frac{\partial}{\partial x}\left(\rho_w q_y\right) dydxdz$ and $-\frac{\partial}{\partial x}\left(\rho_w q_z\right) dzdxdy$. Combining these three terms yields the total accumulation of mass in the controlled volume:

$$-\left(\frac{\partial}{\partial x}\rho_w q_x + \frac{\partial}{\partial y}\rho_w q_y + \frac{\partial}{\partial z}\rho_w q_z\right) dxdydz \qquad (2.6)$$

If the water in the porous media is saturated, then its volume is equal to $ndxdydz$, where *n* (-) is the porosity. The initial mass of the water is thus $\rho_w ndxdydz$. The volume of solid material is $\left(1-n\right) dxdydz$. Any change is the mass of water *M* (kg), with respect to time *t* (s) is given by

$$\frac{\partial M}{\partial t} = \frac{\partial}{\partial t}\left(\rho_w n dx dy dz\right) \tag{2.7}$$

As the pressure in the controlled volume changes, the fluid density will change, and also the porosity of the aquifer. The compressibility of water β is defined as the rate of change in density with regards to pressure, *P* (Pa):

$$\beta dP = \frac{d\rho_w}{\rho_w} \tag{2.8}$$

The aquifer also changes its volume with pressure. Assuming the change is only vertical, the aquifer compressibility, α is given by

$$\alpha dP = \frac{d\left(dz\right)}{dz} \tag{2.9}$$

As the aquifer compresses or expands, the porosity *n*will change, while the volume of the solids, V_s will be constant. Likewise, if the only deformation is in the *z*-direction, $d\left(dx\right)$ and $d\left(dy\right)$ will be equal to zero:

$$dV_s = 0 = d\left[\left(1-n\right)dxdydz\right] \tag{2.10}$$

Differentiation of the above equation yields

$$dzdn = \left(1-n\right)d\left(dz\right) \tag{2.11}$$

and

$$dn = \frac{\left(1-n\right)d\left(dz\right)}{dz} \tag{2.12}$$

The pressure *P* at a point in the aquifer, is equal to $P_0 + \rho_w gh$, where P_0 is atmospheric pressure, and *h*is the height of a column of water above the point. Therefore, $dP = \rho_w gdh$ and Eq. (2.8) and Eq. (2.9) becomes

$$d\rho_w = \rho_w \beta \left(\rho_w g dh \right) \tag{2.13}$$

and

$$d\left(dz\right) = dz\alpha \left(\rho_w g dh \right) \tag{2.14}$$

Eq. (2.12) can be rearranged if $d\left(dz\right)$ is replaced by Eq. (2.14)

$$dn = \left(1-n\right)\alpha \rho_w g dh \tag{2.15}$$

If *dx* and *dy* are constant, the equation for change of mass with time in the control volume Eq. (2.7) can be expressed as

$$\frac{\partial M}{\partial t} = \left[\rho_w n \frac{\partial \left(dz\right)}{\partial t} + \rho_w dz \frac{\partial \left(dn\right)}{\partial t} + ndz \frac{\partial \rho_w}{\partial t} \right] dxdy \tag{2.16}$$

Substitution of Eq. (2.13), Eq. (2.14) and Eq. (2.15) into Eq. (2.16) yields

$$\frac{\partial M}{\partial t} = \left(\alpha \rho_w g + n\beta \rho_w g \right) \rho_w dxdydz \frac{\partial h}{\partial t} \tag{2.17}$$

The net accumulation of material expressed as Eq. (2.16) is equal to Eq. (2.17), the change of mass with time:

$$\left[\frac{\partial \left(q_x\right)}{\partial x} + \frac{\partial \left(q_y\right)}{\partial y} + \frac{\partial \left(q_z\right)}{\partial z} \right] \rho_w dxdydz = \left(\alpha \rho_w g + n\beta \rho_w g \right) \rho_w dxdydz \frac{\partial h}{\partial t} \tag{2.18}$$

From Darcy's Law in Eq. (2.5)

$$\begin{aligned} q_x &= -K \frac{\partial h}{\partial x} \\ q_y &= -K \frac{\partial h}{\partial y} \\ q_z &= -K \frac{\partial h}{\partial z} \end{aligned} \tag{2.19}$$

Substituting these into Eq. (2.18) yields the governing equation of flow in a confined aquifer:

$$K\left(\frac{\partial^2 h}{\partial x^2}+\frac{\partial^2 h}{\partial y^2}+\frac{\partial^2 h}{\partial z^2}\right)=\left(\alpha\rho_w g+n\beta\rho_w g\right)\frac{\partial h}{\partial t} \tag{2.20}$$

which is a general equation for three dimensional flow for an isotropic, homogeneous porous medium. For two-dimensional flow with no vertical components, the storativity, *S* (-), is defined as $S=b\left(\alpha\rho_w g+n\beta\rho_w g\right)$, and transmissivity, $T\left(m^2\,s^{-1}\right)$, is defined as $T=Kb$, where *b*(m) is the aquifer thickness. Therefore, the general equation for two dimensional case is

$$\frac{\partial^2 h}{\partial x^2}+\frac{\partial^2 h}{\partial y^2}=\frac{S}{T}\frac{\partial h}{\partial t} \tag{2.21}$$

Unconfined Aquifer: The general flow equation for two-dimensional unconfined flow is known as the Boussinesq equation:

$$\frac{\partial}{\partial x}\left(h\frac{\partial h}{\partial x}\right)+\frac{\partial}{\partial y}\left(h\frac{\partial h}{\partial y}\right)=\frac{S_y}{K}\frac{\partial h}{\partial t} \tag{2.22}$$

where *h* (m) is the hydraulic head, S_y (1/m) is the specific yield, and *K* is the hydraulic conductivity. If the drawdown in the aquifer is very small compared with the saturated thickness, the variable thickness *h,* can be replaced with the average thickness *b* (m), that is assumed to be constant over the aquifer. Then the Boussinesq equation can be linearized by this approximation to the following form

$$\frac{\partial^2 h}{\partial x^2}+\frac{\partial^2 h}{\partial y^2}+\frac{\partial^2 h}{\partial z^2}=\frac{S_y}{K_b}\frac{\partial h}{\partial t} \tag{2.23}$$

2.3.2 Equations for mass transport

Diffusion: A solute in water will move from an area of greater concentration towards area where it is less concentrated. This process is known as molecular diffusion. Diffusion will occur as long

as a concentration gradient exists, even when the fluid is not moving. The mass of diffusing is proportional to the concentration gradient, which is expressed as the Fick's first law. In one dimension, Fick's first law is

$$F = -D_d \frac{dC}{dx} \tag{2.24}$$

where $F\left(kg\,m^{-2}\,s^{-1}\right)$ is the mass flux of solute per unit area per unit time; $D_d\left(m^2\,s^{-1}\right)$ is the diffusion coefficient; $C\left(kg\,m^{-3}\right)$ is the solute concentration, and *dC/dx* is the concentration gradient. If the concentration changes with time, Fick's second law is applied. In one dimensional form, it is:

$$\frac{\partial C}{\partial t} = D_d \frac{\partial^2 C}{\partial x^2} \tag{2.25}$$

In porous media, diffusion cannot proceed as fast as it can in water because the ions must follow longer pathways as they travel around mineral grains. To account for this, an effective diffusion coefficient, D^* must be used.

$$D^* = \omega D_d \tag{2.26}$$

where ω is the coefficient that is related to the tortuosity. It is an empirical coefficient that takes into account the effect of the solid phase of the porous medium on the diffusion. In laboratory studies of diffusion of the non-adsorbed ions in the porous geologic materials, ω values between 0.5 and 0.01 are commonly observed.

Advection: Dissolved solids are carried along with the flowing ground water. This process is called advective transport, or convection. For one-dimensional flow to a unit cross-sectional area

of the porous media, the quantity of water flowing is equal to the average linear velocity v_x times the effective porosity *n.*

$$v_x = \frac{K}{n}\frac{dh}{dl} \tag{2.27}$$

where $K\left(m\,s^{-1}\right)$ is the hydraulic conductivity. The one-dimensional mass flux, F_x due to advection is equal to the quantity of water flowing times the concentration of dissolved solids and is given as follows

$$F_x = v_x nC \tag{2.28}$$

Hydrodynamic Dispersion: The hydrodynamic dispersion coefficient *D* is represented by the following formulas:

$$D_L = \alpha_L v_i + D^* \tag{2.29}$$

$$D_T = \alpha_T v_i + D^* \tag{2.30}$$

where D_L and D_T are the longitudinal and transverse hydrodynamic dispersion coefficient, with α_L and α_T are longitudinal and transverse dispersivity, respectively,

Advection-Dispersion Equation: According to Bear (1972), the derivation of the advection-dispersion equation is based on the conservation of mass of solute flux into and out of an REV of porous media. As the solute will be transported by advection and hydrodynamic dispersion, the solute transport in *i* direction is given by

Advective transport: $v_i nCdA$ (2.31)

Dispersive transport: $nD_i \frac{\partial C}{\partial t} dA$ (2.32)

where *dA* is the cross-sectional are of the element and *i* direction is normal to that cross-sectional face. The total mass of solute per unit cross-sectional area transported in the *I* direction per unit time, F_i is the sum of the advective and dispersive transport and is given by

$$F_i = v_i nC - nD_i \frac{\partial C}{\partial t} dA \tag{2.33}$$

The negative sign indicates that the dispersive flux is from areas of greater to areas of lesser concentration. The total amount of solute entering the REV is

$$F_x dzdy + F_y dzdx + F_z dxdy \tag{2.34}$$

The total amount of solute leaving the REV is

$$\left(F_x + \frac{\partial F_x}{\partial x} dx \right) dzdy + \left(F_y + \frac{\partial F_y}{\partial y} dy \right) dzdx + \left(F_z + \frac{\partial F_z}{\partial z} dz \right) dxdy \tag{2.35}$$

The difference between the mass of the solute entering the REV and the amount leaving it is

$$-\left(\frac{\partial F_x}{\partial x} + \frac{\partial F_y}{\partial y} + \frac{\partial F_z}{\partial z} \right) dxdydz \tag{2.36}$$

The rate of mass change in the REV is therefore

$$n \frac{\partial C}{\partial t} dxdydz \tag{2.37}$$

By the law of mass conservation, the rate of mass change in the REV must be equal to the difference in the mass of the solute entering and the mass leaving,

$$\frac{\partial F_x}{\partial x} + \frac{\partial F_y}{\partial y} + \frac{\partial F_z}{\partial z} = -n \frac{\partial C}{\partial t} \tag{2.38}$$

Substituting Eq. (3.33) into Eq. (3.38) and cancelling *n* yields

$$\frac{\partial C}{\partial t}=\left[\frac{\partial}{\partial x}\left(D_x\frac{\partial C}{\partial x}\right)+\frac{\partial}{\partial y}\left(D_y\frac{\partial C}{\partial y}\right)+\frac{\partial}{\partial z}\left(D_z\frac{\partial C}{\partial z}\right)\right]-\left[\frac{\partial}{\partial x}\left(v_xC\right)+\frac{\partial}{\partial y}\left(v_yC\right)+\frac{\partial}{\partial z}\left(v_zC\right)\right] \tag{2.39}$$

which is the governing equation for three-dimensional mass transport for a conservative solute, i.e. the solute that does not interact with the porous media or undergo sorption or decay processes. If the Laplace operator is applied, the above equation can be rewritten as,

$$\frac{\partial C}{\partial t}=\nabla\left(D\nabla C\right)-\nabla\left(\vec{v}C\right) \tag{2.40}$$

where $\vec{v}$ is the velocity vector. If the porous media has a sorption effect on the transported chemical component, following Henry's sorption isotherm,

$$C_s=K_D\cdot C \tag{2.41}$$

where $C_s\left(kg\,kg^{-1}\right)$ is the concentration of adsorbed species, $K_D\left(m^3\,kg^{-1}\right)$ is the distribution coefficient. To include this sorption effect, the retardation factor *R* (-) is defined as,

$$R=1+\frac{\rho_b}{n}K_D=1+\frac{1-n}{n}\rho_sK_D \tag{2.42}$$

with ρ_b the bulk density of the media. In this case, the governing equation becomes

$$\frac{\partial C}{\partial t}=\nabla\left(D\nabla C\right)-\nabla\left(\frac{\vec{v}}{R}C\right)-\frac{\rho_b}{R}\frac{\partial C_s}{\partial t} \tag{2.43}$$

If the transported species is radioactive, then a first order decay term also needs to be included.

$$\frac{\partial C}{\partial t}=\nabla\left(D\nabla C\right)-\nabla\left(\frac{\vec{v}}{R}C\right)-\frac{\rho_b}{R}\frac{\partial C_s}{\partial t}-\lambda\cdot C \tag{2.44}$$

2.4 Geochemical Modeling

The formation of complexes between aqueous cations and anions, as well as reactions between aqueous species and their solid or gaseous forms, are described by an equilibrium expression for the relevant geochemical reaction

$$K_{eq} = \frac{(products)}{(reactants)} \tag{2.45}$$

where K_{eq} is the equilibrium constant and the activities of the products and the reactants are designated by parentheses. Databases contained in most geochemical models contain the thermodynamic values of *K* for these equilibrium expressions.

Solute activities (*a*) are related to their concentration through the single-ion activity coefficient (γ)

$$a_i = \gamma_i m_i \quad or \quad a_i = \gamma_i M_i \tag{2.46}$$

where a_i is the activity of a species, m_i is the molality of the species, and M_i is the molarity of the species.

In dilute waters (i.e. ionic strength I < 0.1M), long range electrostatic forces between ions influence the activity of the ions. The effects of these forces on the activity coefficient are adequately described by the extended Debye-Hückel expression

$$\log \gamma_i = -AZ_i^2 \frac{I^{1/2}}{1 + BaI^{1/2}} \tag{2.47}$$

where Z_i is the charge number of the ion, *A* and *B* are the constants determined by the absolute temperature and dielectric constant of the system, *a* is an adjustable size parameter corresponding roughly to the radius of the hydrated ion, and *I* is the ionic strength.

The Debye-Hückel expression does not account for all interactions among solutes. This limits the ability of the model to accurately predict activity coefficients of simple electrolytes at higher ionic strengths. A variety of empirical and semi-empirical expressions have been proposed to extend the applicability of the Debye-Hückel equation to higher ionic strength systems including the Davies equation shown below

$$\log \gamma_i = -0.512 Z_i^2 \left(\frac{I^{1/2}}{1+I^{1/2}} - 0.3I \right) \tag{2.48}$$

The general reaction for two component dissolution is shown below for metals/cations, M^{m+}, and ligands, L^{l-}, from which we can define the equilibrium dissolution constant, K_{dis}

$$\begin{aligned} M_a L_b (s) &= a M^{m+}(aq) + b L^{l-}(aq) \\ K_{dis} &= \frac{\left(M^{m+}\right)^a \left(L^{l-}\right)^b}{M_a L_b} \end{aligned} \tag{2.49}$$

where *a* and *b* are stoichiometric coefficients, and m^+ and l^- are the charges of the ions. The solubility product constant, K_{so} is defined as

$$K_{so} = K_{dis}\left(M_a L_b\right) \tag{2.50}$$

The ion activity product, IAP is defined as

$$IAP \equiv \left(M^{m+}\right)^{a}\left(L^{l-}\right)^{b} \tag{2.51}$$

The relative saturation, Ω, is defined as

$$\Omega = \frac{IAP}{K_{so}} \tag{2.52}$$

The relative saturation can be monitored over time to assess the degree of equilibration in a system. If $\Omega < 1$, then the system is undersaturated with respect to the solid. If $\Omega > 1$, then the system is oversaturated with respect to the solid. Finally if $\Omega = 1$, then the system is in equilibration with respect to the solid.

The degree of equilibrium with respect to the precipitation/dissolution of a particular mineral can also be calculated using the saturation index, SI.

$$SI = \log\left[\frac{IAP}{K_{so}}\right] \tag{2.53}$$

Like the relative saturation, if the SI < 0, then the system is undersaturated. If the SI > 0, then the system is oversaturated, while if SI » 0, then the system is at equilibrium.

Chapter 3

Literature Review

The use of MICP for soil improvement purpose is a relatively new concept. During recent years small and large scale laboratory and field experiments have been carried out to investigate its applicability. Very few article exist in literature proposing a suitable numerical model for biogrout. This chapter does a thorough review of the available literature from both experimental and numerical model perspective.

3.1 Biogrout Experiment

Stocks-Fischer et al. (1999) examined physical and biochemical properties of $CaCO_3$ precipitation induced by Bacillus pasteurii, an alkalophilic soil microorganism. X-ray diffraction analysis quantified the composition of the mineral deposited in sand and identified the $CaCO_3$ crystal as calcite. Examination by scanning electron microscopy identified bacteria in the middle of calcite crystals, which acted as nucleation sites. The rate of microbiological $CaCO_3$

precipitation correlated with cell growth and was significantly faster than that of chemical precipitation. Biochemical properties of urease (urea amidohydrolase, E.C. 3.5.1.5) from B. pasteurii that was indirectly involved in $CaCO_3$ precipitation were examined to understand the kinetics of the microbiological process. Urease from B. pasteurii exhibited a relatively low affinity for urea at pH 7.0 with a K_m of 41.6 mM and $V_{\max}$ of 3.55 $mM\,\min^{-1}\,mg^{-1}$ protein and increased affinity at pH 7.7 with a K_m of 26.2 mM and $V_{\max}$ of 1.72 $mM\,\min^{-1}\,mg^{-1}$ protein. Results of kinetic studies indicate that urease activity and its affinity to urea are significantly high at the pH where calcite precipitation is favorable. Their findings further suggest a potential use of the microbial calcite precipitation process in remediation of the surface and subsurface of porous media.

Whiffin et al. (2007) conducted experiment where a five meter sand column was treated with bacteria and reagents under conditions that were realistic for field applications, in order to evaluate MCP as a soil strengthening process. The injection and reaction parameters were monitored during the process and both bacteria and process reagents could be injected over the full column length at low pressures (hydraulic gradient <1; a flow rate of approximately 7 m/day) without resulting in clogging of the material. After treatment, the column was subjected to mechanical testing, which indicated a significant improvement of strength and stiffness over several meters. Calcium carbonate was precipitated over the entire five meter treatment length. Improvement of the load bearing capacity of the soil without making the soil impermeable to fluids was shown with microbial carbonate precipitation, and this is a unique property compared to alternative soil treatment methods that are currently available for use in the subsurface.

DeJong et al. (2006) presented the results of a study in which natural microbial biological processes were used to engineer a cemented soil matrix within initially loose, collapsible sand. Microbially induced calcite precipitation (MICP) was achieved using the microorganism Bacillus pasteurii, an aerobic bacterium pervasive in natural soil deposits. The microbes were introduced to the sand specimens in a liquid growth medium amended with urea and a dissolved calcium source. Subsequent cementation treatments were passed through the specimen to increase the cementation level of the sand particle matrix. The results of both MICP- and gypsum-cemented specimens were assessed nondestructively by measuring the shear wave velocity with bender elements. A series of isotropically consolidated undrained compression (CIUC) triaxial tests indicate that the MICP-treated specimens exhibit a noncollapse strain softening shear behavior, with a higher initial shear stiffness and ultimate shear capacity than untreated loose specimens. This behavior is similar to that of the gypsum-cemented specimens, which represent typical cemented sand behavior. SEM microscopy verified formation of a cemented sand matrix with a concentration of precipitated calcite forming bonds at particle-particle contacts. X-ray compositional mapping confirmed that the observed cement bonds were comprised of calcite.

van Paassen (2009) in his PhD thesis entitled ‘Biogrout: ground improvement by microbially induced carbonate precipitation’ submitted to TU Delft, has conducted a series of laboratory and field scale experiments. He described methods in which bacteria and reagents are flushed sequentially through the soil in order to achieve a more efficient use and homogeneous distribution of the bacteria and the resulting precipitation rate over a long distance. 5m sand column experiment provided the first evidence that significant strength increase could be achieved at low injection pressure, within 3 days of treatment and 5 flushed pore volumes

(including placement of bacteria and removing the remaining ammonium chloride), at a long distance and without reducing the permeability significantly. First scale-up experiment was performed in a $1\,m^3$ container set-up simulating a spherical injection from a single point and secondly the results are presented from a 100 m^3 field scale experiment. While analyzing the results of these scale-up experiments, empirical relations could be established between the amount of $CaCO_3$ and engineering parameters, like density, strength, stiffness, porosity and permeability. These correlations enabled to determine the required parameters and to design treatment procedures for several emphasized applications. The feasibility of using Biogrout for the in-situ reinforcement of calcarenite room and pillar mines was investigated, showing that Biogrout can also be used to increase the strength in already lightly cemented rocks. Remaining issues in the Biogrout process based on urea hydrolysis include the required removal of ammonium chloride and the use of axenically cultivated aerobic organisms with consequent decaying urease activity in time due to a lack of oxygen in the subsurface. To avoid both these issues the suitability of other possible MICP processes for ground improvement is evaluated. The feasibility of the best alternative, in which calcium acetate (or another fatty acid) and calcium nitrate are converted to induce calcium carbonate precipitations is evaluated experimentally.

3.2 Biogrout Numerical Simulation

van Wijngaarden et al. (2011) proposed the mathematical modeling of biogrout: a new ground improvement technique based on Microbial Induced Carbonate Precipitation. The model contains the concentrations of the dissolved species that are present in the biochemical reaction.

These concentrations has been solved from an advection dispersion reaction equation with a variable porosity.

van Wijngaarden et al. (2011) proposed the mathematical modeling of biogrout: a new ground improvement technique: extension to 3D. A mathematical model was created to describe the process. The model contains concentration of the dissolved species that are present in the precipitation reaction. These concentrations can be solved from a convection-dispersion-reaction equation with a variable porosity. Other model equations involve the concentrations of the bacteria and of the solid sodium carbonate, the decreasing porosity due to precipitation and the flow. The partial differential equations are solved by the Standard Galerkin Finite Element Method. The subject of this paper is the extension of the mathematical model to 3D.

van Wijngaarden et al. (2012) proposed a model containing three phases of bacteria. bacteria in suspension, adsorbed bacteria and fixed bacteria. An analytical solution is derived for instantaneous reactions between these three phases. The analytical solution is compared to numerical simulations for finite reaction rates. For the numerical simulations the standard Galerkin Finite Element Method is used.

van Wijngaarden et al. (2013) explained that nutrients and the side product of microorganism reactions that are dissolved in water cause the fluid to be denser than water Moreover, the density changes as a result of the varying composition. This changing density has a significant impact on the flow. Since the composition and hence, the density is not known beforehand, a careful choice of the (pressure) boundary conditions, especially on the outflow boundary, is needed. In this article, several methods to approximate the pressure on the outflow boundary are compared. The method that they propose also works for an unstructured mesh, which gives a larger freedom in the mesh generation.

Laloui et al. (2011) proposed a mathematical model accounting for the bio-hydro-mechanical couplings existing between fluid flow, bacterial concentration evolution, exchanges between phases, transport and miscibility. Finite element modeling of column injection tests is carried out to validate the formulation and to demonstrate the potentiality of the developed model.

Fauriel and Laloui (2012) carried out a comprehensive research study to better understand and describe the coupled phenomena of multispecies reactive biogrout transport in a saturated, deformable soil. A unique predictive model of the behavior of the porous media during biogrout injection is presented. The general field equations describing the system are derived from the macroscopical balance equations and constitutive equations. The set of field equations is numerically discretized. Finally, numerical examples are provided as a first step to validate the capabilities of the proposed model.

Barkouki et al. (2011) showed that microbially induced calcite precipitation (MICP) offers an alternative solution to a wide range of civil engineering problems. They have conducted laboratory tests to show that MICP can immobilize trace metals and radionuclides through co-precipitation with calcium carbonate. MICP has also been shown to improve the undrained shear response of soils and offers potential benefits over current ground improvement techniques that may pose environmental risks and suffer from low "certainty of execution." Their objective is to identify an effective means of achieving uniform distribution of precipitate in a one-dimensional porous medium. Their approach involves column experiments and numerical modeling of MICP in both forward and inverse senses, using a simplified reaction network, with the bacterial strain Sporoscarcina pasteurii. It was found that the stop-flow injection of a urea- and calcium-rich solution produces a more uniform calcite distribution as compared to a continuous injection

method, even when both methods involve flow in opposite direction to that used for bacteria cell emplacement. Inverse modeling was conducted by coupling the reactive transport code TOUGHREACT to UCODE for estimating chemical reaction rate parameters with a good match to the experimental data. It was found, however, that the choice of parameters and data was not sufficient to determine a unique solution, and our findings suggest that additional time and space-varying analytical data of aqueous species would improve the accuracy of numerical modeling of MICP.

Martinez et al. (2014) demonstrated the utility of a simple bio-geochemical reactive transport model to predict MICP in one-dimensional column experiments. The mathematical model was originally developed in the framework of the TOUGHREACT code to include kinetically controlled reaction rates for urea hydrolysis and calcite precipitation. Inverse modeling, via UCODE-2005, is utilized to calibrate and verify the model to experimental data including aqueous and mineral chemistry. Results indicate good agreement between data and simulated results for capturing the trends and magnitudes of a variety of MICP treatment schemes in half meter, one-dimensional flow columns. A design procedure is presented for predicting MICP in one-dimensional flow by sequentially coupling UCODE-2005 with TOUGHREACT.

Elena Shigorina (2014) in her master's thesis, University of Struttgart, Germany, has presented a numerical model for microbially induced calcite precipitation (MICP) on a large, realistic spatial 3 D scale investigating the influence of different injection schemes on the distribution of precipitated calcite within the porous media. In this work, a multi-compositional two phase model was used, based on the simulator DuMux. The applied model describes the physical and chemical process during the different injections. The results show that the reduction of permeability can be manipulated using different injection schemes.

3.3 Critical Review

van Wijngaarden et al. (2011)selected the model domain as 1m. Their result show that for half of the column length porosity and permeability decrease is significant and for the other half it is negligible. From Whiffin et al. (2007), van Paassen (2009) and Barkouki et al. (2011) experiments it is observed that they have obtained precipitation throughout the entire column. For small length column the distribution of calcite over the length of column is homogeneous. van Wijngaarden et al. (2011) model fails to explain this event.

Barkouki et al. (2011) presented 0.5m small scale experimental numerical simulation of the same experiment. This kind of experiment and simulation are important to understand the process better as well as to experimentally validate the developed model.

Elena Shigorina (2014) developed a finite difference model of MICP, but the aim of that model was to use MICP as a sealing material, and not as a soil improvement technique.

Chapter 4

Concept of the Developed Model

This chapter presents several aspects of the developed numerical model.

4.1 Main Assumptions

- Only dissolved species react.
- The reaction consists of a hydrolysis reaction and a precipitation reaction; sorption of components and decay of bacterial growth is neglected.
- The biochemical reaction of the Biogrout process is governed by reaction (2.1) and is also assumed to take place instantaneously.
- Calcium carbonate is not transported but it precipitates on the matrix of the porous medium
- The fluid is incompressible.

- The hydrolysis of urea and the precipitation of calcium carbonate have no influence on the total volume of the fluid over the entire domain of computation.
- Fluid viscosity and density is constant.
- Kinetic constants are independent of initial biomass, urea and Ca^{2+} concentration.

4.2 Simulation code OpenGeoSys-PhreeqC

The open source scientific code OpenGeoSys (OGS), developed for the simulation of coupled multiphase flow and reactive transport processes in the subsurface (Kolditz and Bauer 2004; Wang and Kolditz 2007; Kolditz and Shao 2009; Graupner et al. 2011; Kolditz et al. 2012) has been applied to a variety of reactive transport problems in porous media (e.g. Bauer et al. 2006; Beyer et al. 2006, 2009; Park et al. 2008; Shao et al. 2009; Xie et al. 2006). To account for the reactive interactions between fluid and solid (mineral) phases, OGS offers interfaces to several different geochemical reaction simulators.

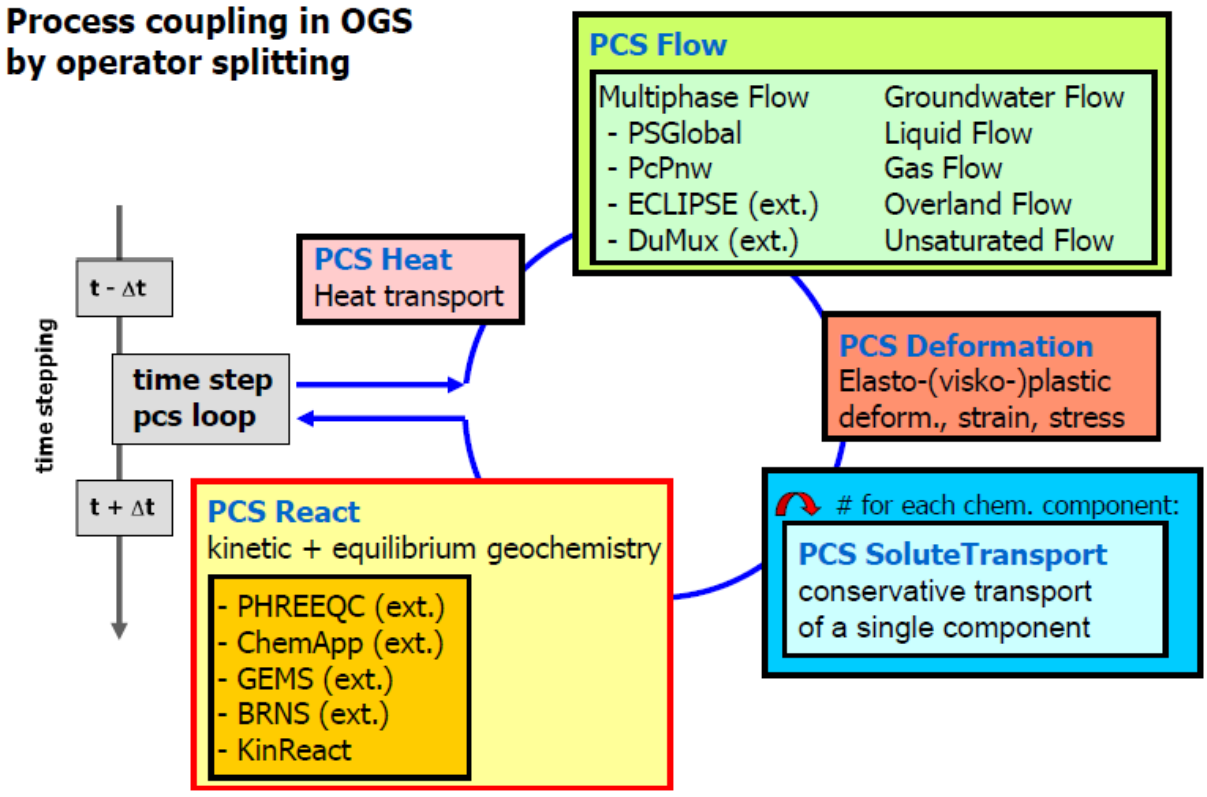

Fig. 4.1: Coupling scheme of OpenGeoSys with geochemical codes (Kolditz et al. 2012)

PHREEQC is a geochemical speciation code based on the Law of Mass Action (LMA) approach (Parkhurst and Appelo, 1999). It differentiates between master species, whose concentrations directly enter into mass-conservation equations, and secondary species, whose concentrations are found through the LMA expressions using master species activities and equilibrium constants of formation reactions. During the calculation, the total balance quantities of the master species are given as system mass balance constraints. This allows the solution of the mass-conservation equations iteratively together with the LMA expressions using a Newton–Raphson or a similar numerical algorithm. The coupled OGS–PhreeqC simulator (Xie et al. 2006) employs a

sequential operator splitting scheme to solve the coupled processes during a simulation time step (Fig.4.1).

First, flow of all mobile phases and conservative multi-component transport are simulated by OGS using a Galerkin finite element method to solve the system of partial differential equations. Subsequently, fluid and mineral phase reactive interactions are quantified. Concentrations of all transported species have to be expressed in weight units, i.e. in mol per kg of solid phase. PhreeqC, however, expects input of total moles of all species of the geochemical system per unit weight of aquifer. Hence, a conversion of units is necessary before and after data exchange between OGS and PhreeqC, respectively.

4.3 Different Injection Schemes

Biogrout process simulation has been done according to two different injection schemes: 2-phase and 1-phase schemes. In 2-phase scheme, in the first shot, bacteria and urea has been injected and sufficient time has been allowed for urea hydrolysis to take place and the domain to be filled with carbonate ion. In the second shot, calcium cation is injected. In 1-phase scheme, it is assumed that all the reactants; urea, bacteria and calcium have been injected simultaneously and hence no seating time is provided. Table 4.1-4.4 shows the duration and concentration of different components during 2-phase and 1-phase scheme for both 0.5m and 1m domain, respectively.

Table 4.1: 2-Phase scheme for 0.5m domain

Injection	Duration (hour)	Concentration (mol/kgw)
Urea-rich	2.8	50
Groundwater flow	46.7	0
No-flow	46.7	0
Calcium-rich	2.8	15
Groundwater flow	23.3	0
Total	122.3	

Table 4.2: 2-Phase scheme for 1m domain

Injection	Duration (hour)	Concentration (mol/kgw)
Urea-rich	5.6	50
Groundwater flow	46.7	0
No-flow	46.7	0
Calcium-rich	5.6	15
Groundwater flow	23.3	0
Total	127.9	

Table 4.3: 1-Phase scheme for 0.5m domain

Injection	Duration (hour)	Concentration (mol/kgw)
Urea+Calcium-rich	2.8	50(urea)+15(calcium)
Groundwater flow	23.3	0
Total	26.1	

Table 4.4: 1-Phase scheme for 1m domain

Injection	Duration (hour)	Concentration (mol/kgw)
Urea+Calcium-rich	5.6	50(urea)+15(calcium)
Groundwater flow	23.3	0
Total	28.9	

4.4 Boundary conditions and Meshing

Dirichlet boundary conditions have been applied throughout. For mass transport with concentration input, $c = c_{in}$ at $x = 0$, c_{in} =input concentrations as mentioned in the injection schemes. At $x = 0.5$ or $x = 1$, an outflow boundary condition is assumed. For groundwater flow, initially in the domain there is a head of 1m. Boundary condition is at $x = 0$, head = 10000m.

Meshing has been done with linear elements using pre-processing software GINA.

4.5 Kinetics of Urea Hydrolysis and Calcite Precipitation

2-phase Scheme: For urea hydrolysis the following kinetic equation was considered:

$$\frac{d[urea]}{dt} = -k_{urea} \cdot [urea] \cdot X \tag{4.1}$$

Urea hydrolysis rates were calculated under the assumption that the reaction is zero order with respect to biomass $(X = 1)$

It is assumed that for every mole of urea getting degraded, 1mole of CO_3^{2-} and 2 moles of NH_4^+ is produced.

Therefore, the rate of production of CO_3^{2-} can be written as

$$\frac{d[CO_3^{-2}]}{dt} = k_{urea} \cdot [urea] \tag{4.2}$$

The rate of calcite precipitation is calculated according to Palandri and Kharaka (2004).

$$\frac{d[CaCO_3]}{dt} = -SA\left[\begin{array}{l} k_{acid}^{298.15K} \exp\left(\frac{-E_{acid}}{R}\left(\frac{1}{T} - \frac{1}{298.15K}\right)\right)\prod a_i^{n_1^i}\left(1-\Omega^{p_1}\right)^{q_1} \\ +k_{neutral}^{298.15K} \exp\left(\frac{-E_{neutral}}{R}\left(\frac{1}{T} - \frac{1}{298.15K}\right)\right)\prod a_i^{n_2^i}\left(1-\Omega^{p_2}\right)^{q_2} \\ +k_{base}^{298.15K} \exp\left(\frac{-E_{base}}{R}\left(\frac{1}{T} - \frac{1}{298.15K}\right)\right)\prod a_i^{n_3^i}\left(1-\Omega^{p_3}\right)^{q_3} \end{array}\right] \tag{4.3}$$

$k_{acid}, k_{neutral}, k_{base}\left(mol\, m^{-2}\, s^{-1}\right)$ are rate constants for a temperature of 298.15 *K*, $E_{acid}, E_{neutral}, E_{base}\left(J\, mol^{-1}\right)$ are corresponding activation energy terms to describe temperature

T(K) dependence, $R\left(J\,mol^{-1}\,K^{-1}\right)$ is the gas constant, $a_i\left(-\right)$ is the activity of the species *i*, $\Omega\left(-\right)$ is the mineral saturation index, and $n_i, p_i, q_i\left(-\right)$ are empirical constants.

Setting the reaction order n_i to 0 ("zero") allows to remove the dependency on reaction activities from single terms. By setting appropriate parameter values to 1 or 0, it is easily possible to mimic other (simpler) rate laws.

Several models for calculating the reactive surface area $SA\left(m^2\right)$ of a mineral *i* are implemented. The simplest form relates the surface area to the volume of a mineral phase:

$$SA = V_i a_i \tag{4.4}$$

where $V_i\left(m^3\right)$ is the volume of the mineral and $a_i\left(m^2\,m^{-3}\right)$ is the relative surface area per volume.

In this study the reactive surface area for calcite is taken as 0.01 m^2 and other parameters are obtained from Palandri and Kharaka (2004), which are listed in Table 4.5.

Table 4.5: Kinetic parameters used for calcite precipitation (from Palandri and Kharaka (2004))

Mineral phase	Molar weight $\left[kg\,mol^{-1}\right]$	Density $\left[kg\,m^{-3}\right]$	Acid mechanism			Neutral mechanism		Carbonate mechanism		
			logk	*E*	*n*	*logk*	*E*	*logk*	*E*	*n*
Calcite	0.100	2710	-0.30	14	1.000	-5.8	23.5	-3.5	35	1.000

.

1-Phase Scheme: A first order differential equation was assumed for calcite precipitation, assuming that for every mole of Ca^{2+} removed from solution one mole of $CaCO_3$ is formed:

$$\frac{d\left[Ca^{2+}\right]}{dt} = -k_{precip} \cdot \left[Ca^{2+}\right] \tag{4.5}$$

Rate constants were found in literatures which were determined using the least square fit method on Microsoft Excel.

k_{urea} and k_{precip} parameter values are obtained from Stocks-Fischer et al., 1999, Fujita et al., 2000 and Ferris et al., 2003. In order to accurately compare the kinetic parameters of the experiments, the kinetic coefficients were re-evaluated according to Equations 4.2 and 4.5. The initial cell concentration for each experiment also had to be standardized, as some were reported as optical densities (Fujita et al., 2000 and Ferris et al., 2003) and some were reported as CFU/mL (Stocks-Fischer et al., 1999). Table 4.6 shows the re-evaluated data for the experiments (Parks, 2009). This study is carried out using coefficients from Ferris et al., 2003.

Table 4.6: Summary of kinetic coefficients for experiments performed in the literature (Parks, 2009)

	Stocks-Fischer et al. (1999)	Fujita et al. (2000)	Ferris et al. (2003)
S. pasteurii strain	ATCC 6453	ATCC 11859	ATCC 11859
Temperature (°C)	25	20	20
Initial pH	8	6.5	6.5
$\left[Ca^{+2}\right]_0$ (mM)	25.2	25	1.75
$\left[Urea\right]_0$(mM)	333	333	6
$k_{urea}\left(hr^{-1}\right)$	0.0282	0.0081	0.0381
$k_{precip}\left(hr^{-1}\right)$	0.116	0.113	0.014

4.6 Porosity-Permeability Update

Dissolution or precipitation of an assemblage of *i* minerals will result in modifications of the total solid volume fraction within the REV. Hence, after quantification of mineral reactions, the evolution of porosity due to a changed mineral phase volume fraction is evaluated and updated for the next time step $t+\Delta t$ by

$$n\left(t+\Delta t\right)=n\left(t\right)+\left[1+n\left(t\right)\right]\sum_{i=1}^{m}\left[M_i\left(t\right)-M_i\left(t+\Delta t\right)\right]\frac{w_i^{mol}}{\rho_i} \tag{4.6}$$

where $w_i^{mol}\left[kg\,mol^{-1}\right]$ is the molar weight of mineral *i*, $\rho_i\left[kg\,m^{-3}\right]$ the respective density and *m* the number of minerals. The resulting changes in permeability $K\left[m^2\right]$ can be quantified, e.g. by the Kozeny–Carman equation

$$K\left(t+\Delta t\right)=K_0\left(\frac{1-n_0}{1-n\left(t+\Delta t\right)}\right)^2\left(\frac{n\left(t+\Delta t\right)}{n_0}\right)^3 \tag{4.7}$$

where $n_0\left(-\right)$ and $K_0\left(m^2\right)$ are initial porosity and permeability, respectively.

In this study *m*=1, i.e. calcite.

4.7 Execution steps for coupled code OpenGeoSys-PhreeqC

- Domain geometry is defined and domain is discretized into finite elements and nodes.
- Initial and boundary condition of the processes are defined
- Advection-dispersion equation is solved at each node for each time step
    - head at each node is obtained (to calculate flow velocity)
    - concentrations of components are obtained
- These concentrations are transferred from OGS to PhreeqC to calculate chemical reactions at each node
- Updated concentrations of reactants and products are sent back to OGS
- Updated porosity (n) is calculated using the below formula

n(t) = n(t-1)+DV ; DV=[C(t-1)-C(t)] * MW / MD * [1-n(t-1)] (4.8)

MW = molar weight

MD = mineral density

- Permeability is updated from the new porosity according to Kozeny-Carman equation

$$K(t) = K_0 \left(\frac{1-n_0}{1-n(t)} \right)^2 \left(\frac{n(t)}{n_0} \right)^3 \tag{4.9}$$

- With this new updated porosity, permeability and concentration, advection-dispersion equation is solved for the next time step
- The above process is repeated for every time step

4.8 Model Parameters

In this study a one-dimensional domain is considered and simulation has been carried out for two different lengths of the domain. These one-dimensional domains correspond to one-dimension column experiments for bio-grout. The various geotechnical and geochemical parameters considered in this study are listed in Table 4.7.

Table 4.7 : Model parameters

Symbol	Parameter	Value	Unit
ϕ	Initial porosity	0.4	-
K	Initial permeability	1.16E-12	m^2
ρ	Density of groundwater	1000	kg/m^3
η	Viscosity of groundwater	0.001	Pa.s

α_L	Longitudinal dispersivity	0.1	m
α_T	Transverse dispersivity	0.01	m
			m^2/s
D_{a1}	Diffusion coefficient of Ca^{2+}	7.00E-10	
D_{a2}			m^2/s
	Diffusion coefficient of CO_3^{2-}	8.00E-10	
D_{a3}	Diffusion coefficient of urea	1.38E-09	m^2/s
ω	Tortuosity	1	-
h_A	Initial groundwater flow head throughout the domain	1.00E+00	m
h_B	Boundary groundwater flow head at Point0	1.00E+04	m

Chapter 5

Results

5.1 Column Experiment Simulation

Biogrout propagation in a 1-D domain is simulated using the open source coupled software OpenGeoSys-PhreeqC. Two different domains were considered: the small domain and the large domain. Both domains represent similar one-dimensional column. The so called small domain has a length of 0.5m. The length of the big simulation domain is equal to 1m. Boundary conditions are equal for both domains. Fig. 5.1 shows the schematic diagram of the domain.

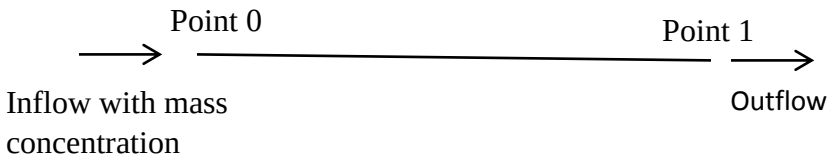

Fig. 5.1: Schematic Diagram of the Simulation Domain

5.2 2-Phase Scheme

Biogrout process is simulated on both the small and the large simulation domains according to injections as specified in the 2-phase injection scheme. The total duration is 122.3 hours for 0.5m domain and 127.9 hours for 1m domain.

5.2.1 Results for Urea Concentration

Figure 5.2 displays the concentration of urea as a function of the position in the column at several times, for both 0.5m and 1m column.

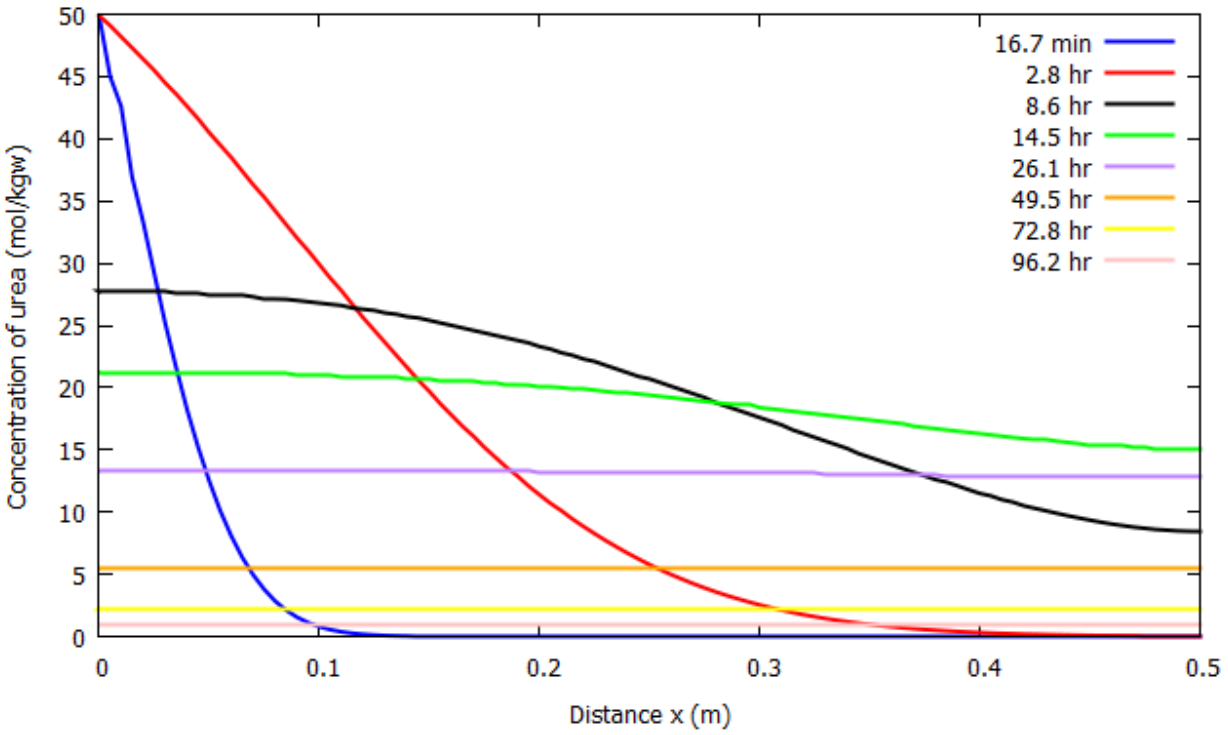

Fig. 5.2 (a): The urea concentration as a function of distance at several times for 2-phase injection scheme, for 0.5m column

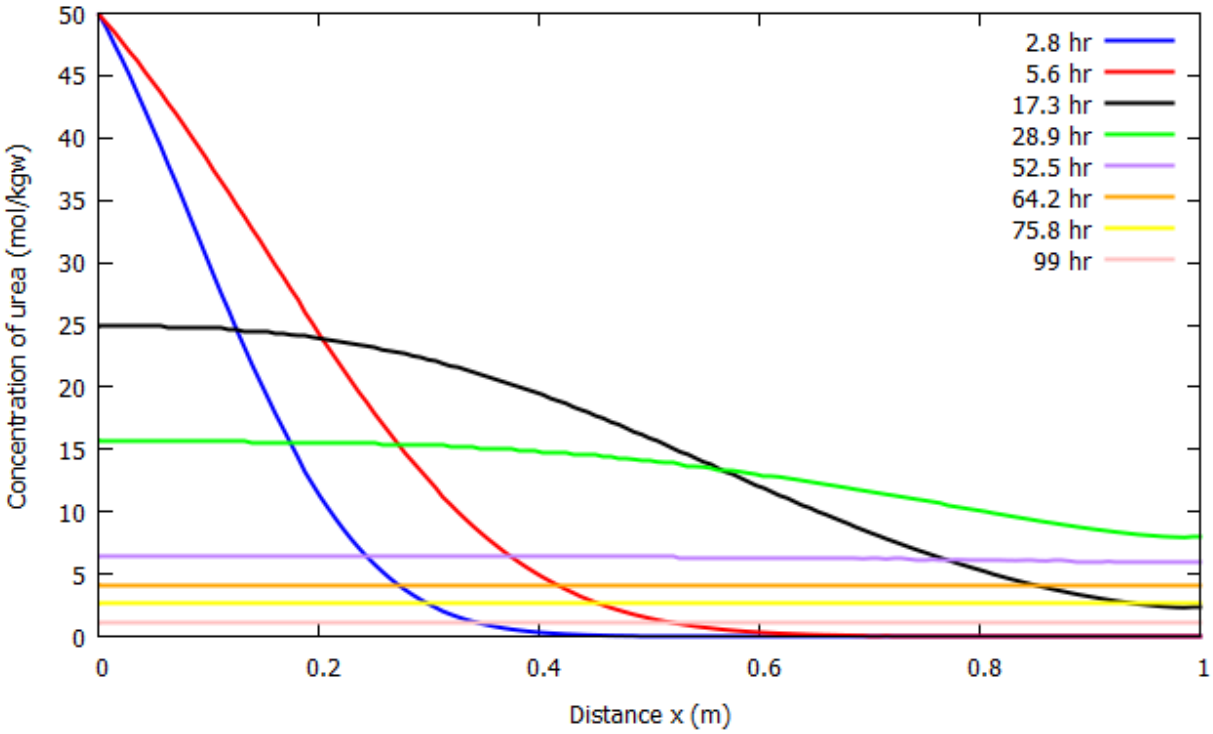

Fig. 5.2 (b): The urea concentration as a function of distance at several times for 2-phase injection scheme, for 1m column

From Fig. 5.2(a), for 0.5m column, it is seen that up to 2.8 hours there was a constant supply of urea, so the concentration of urea at various points is increasing. From 2.8 hour to 26.1 hour, there was no urea injection; only groundwater flow was taking place. So, during this time urea is further getting propagated from higher concentration to lower concentration and at the same time getting degraded into ammonium and carbonate ion. Hence, urea concentration is decreasing at various points during this time. At time 26.1 hour, it is seen that the entire column is filled with equal amount of urea. Between 26.1 hour and 96.2 hour there was no flow, so that the remaining urea can be hydrolyzed. During this time the amount of urea is further decreasing. It is seen that at 96.2 hour, very few urea is left in the column. All have been hydrolyzed into ammonium and carbonate.

Similarly, from Fig. 5.2(b), for 1m column, it is seen that up to 5.6 hours there was a constant supply of urea, so the concentration of urea at various points is increasing. From 5.6 hour to 52.5 hour, there was no urea injection; only groundwater flow was taking place. So, during this time urea was further getting propagated from higher concentration to lower concentration and at the same time getting degraded into ammonium and carbonate ion. Hence, urea concentration is decreasing at various points during this time. At time 52.5 hour, it is seen that the entire column is filled with equal amount of urea. Between 52.5 hours and 99 hours there was no flow, so that the remaining urea can be hydrolyzed. During this time the amount of urea is further decreasing. It is seen that at 99 hour, very few urea is left in the column. All have been hydrolyzed into ammonium and carbonate.

5.2.2 Results for Calcium Carbonate, Porosity and Permeability

Figure 5.3 shows the total amount of calcium carbonate in the domain for 0.5m and 1m column respectively.

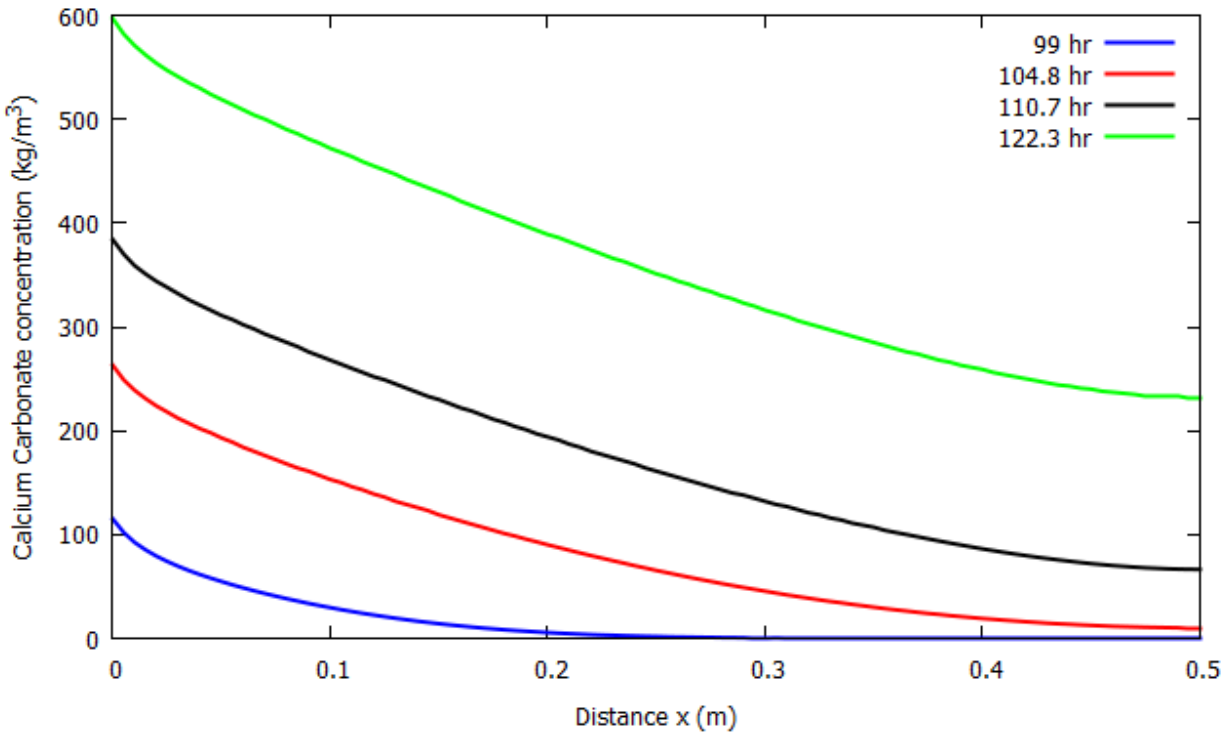

Fig. 5.3 (a): The concentration of calcium carbonate as a function of distance at several times for 2-phase injection scheme, for 0.5m column

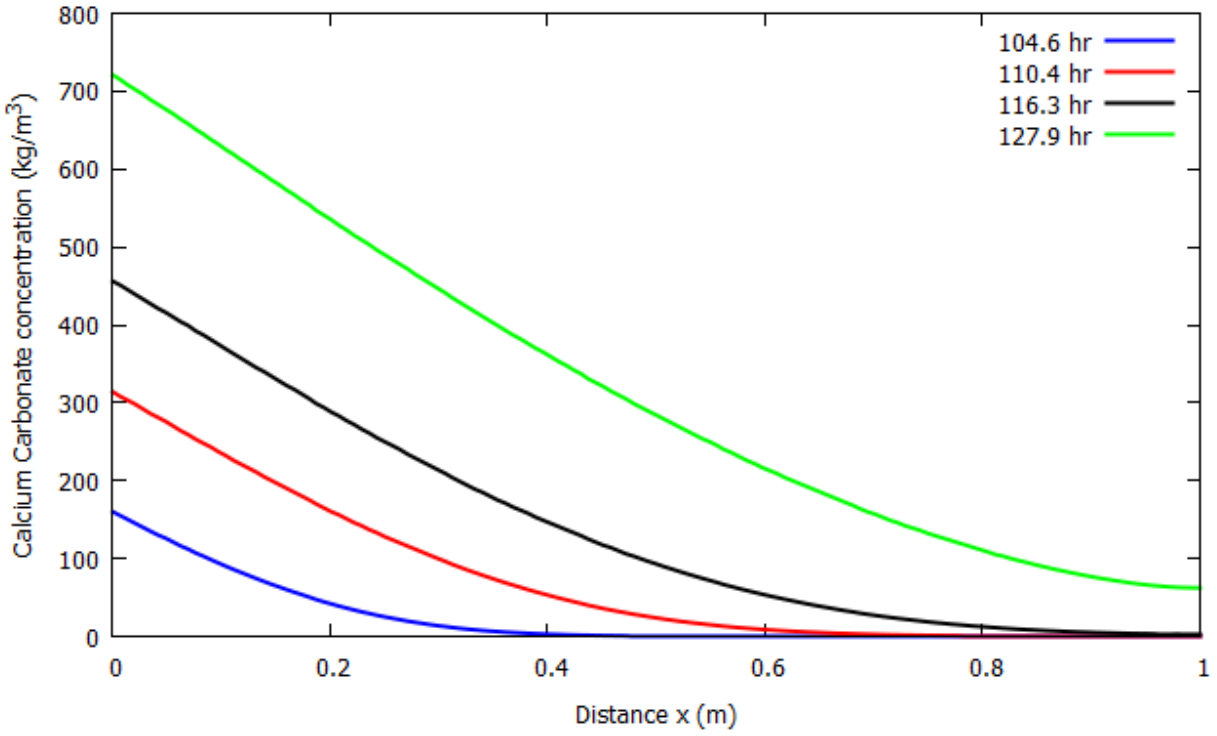

Fig. 5.3 (b): The concentration of calcium carbonate as a function of distance at several times for 2-phase injection scheme, for 1m column

For 0.5m column, after 99 hours, injection of Ca^{2+} is stopped. So from Fig. 5.3(a), the curve corresponding to 99 hour is the amount of calcite precipitated during Ca^{2+} injection period. Between 99 hours and 122.3 hours, calcite precipitation increases throughout the domain as a result of Ca^{2+} propagation and kinetic reaction taking place throughout the domain.

For 1m column, after 104.6 hours, injection of Ca^{2+} is stopped. So from Fig. 5.3(b), the curve corresponding to 104.6 hour is the amount of calcite precipitated during Ca^{2+} injection period. Between 104.6 hours and 127.9 hours, calcite precipitation increases throughout the domain as a result of Ca^{2+} propagation and kinetic reaction taking place throughout the domain.

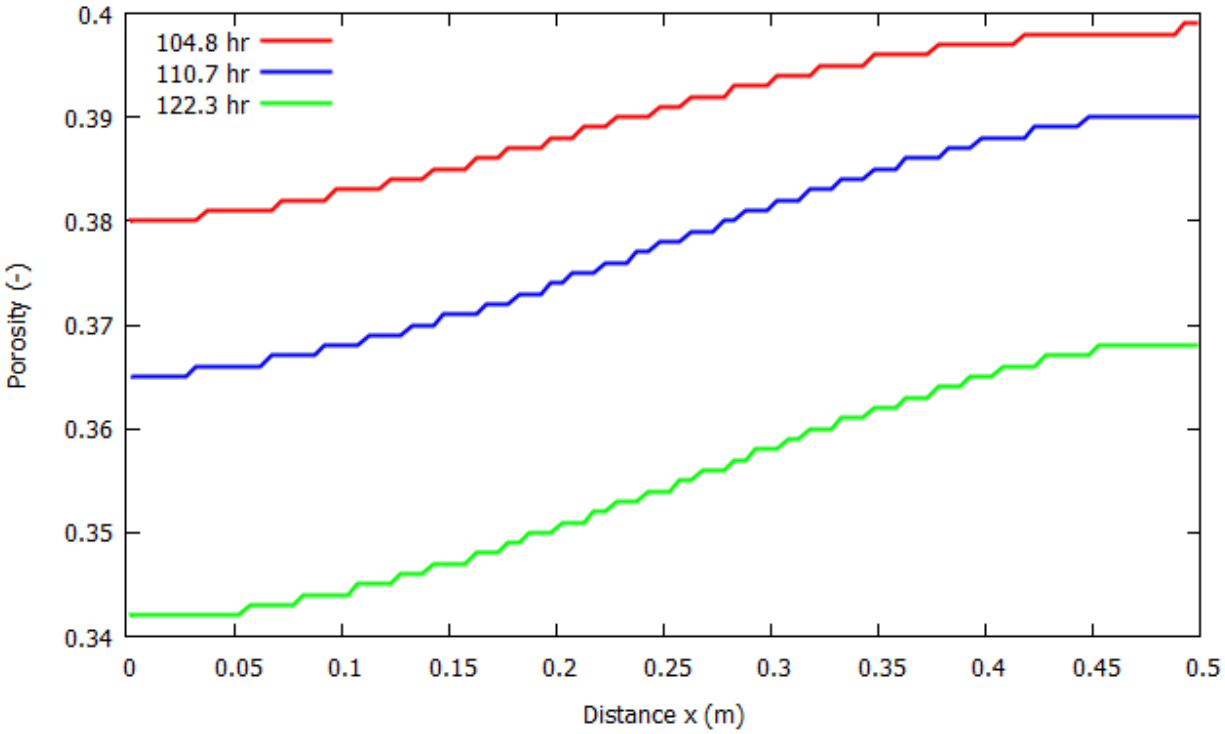

Fig. 5.4 (a): The porosity as a function of distance at several times for 2-phase injection scheme, for 0.5m column

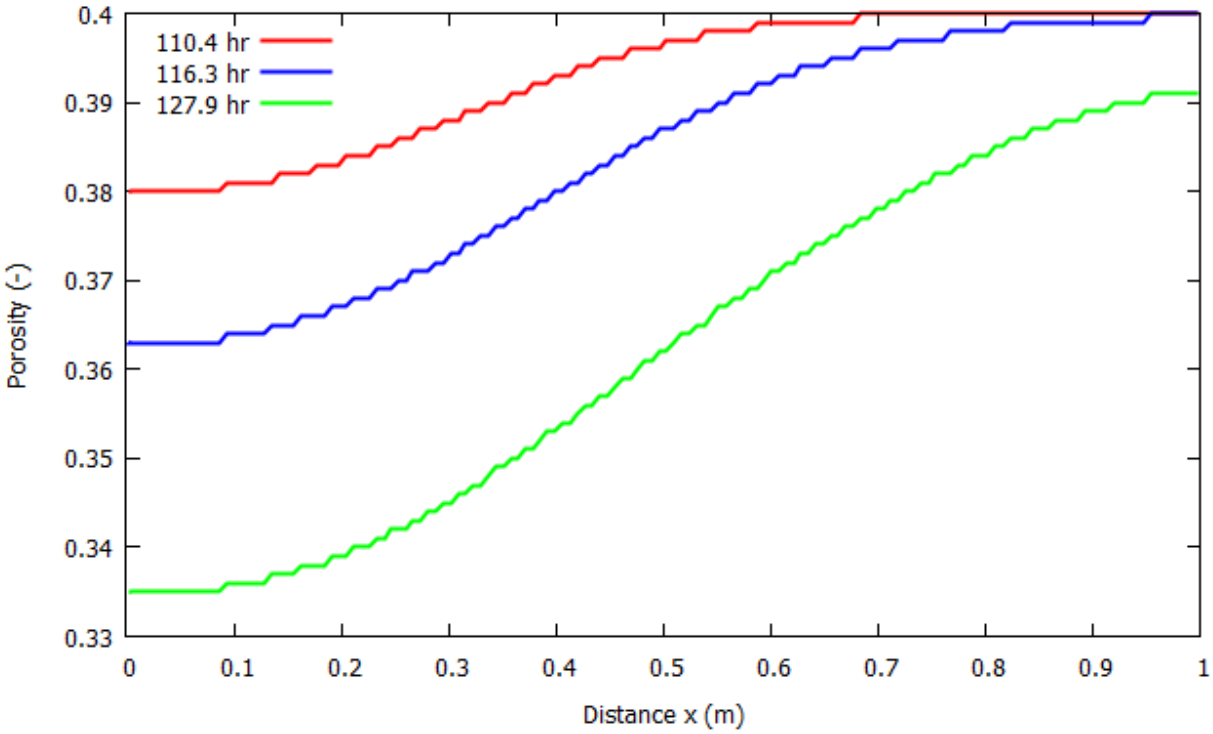

Fig. 5.4 (b): The porosity as a function of distance at several times for 2-phase injection scheme, for 1m column

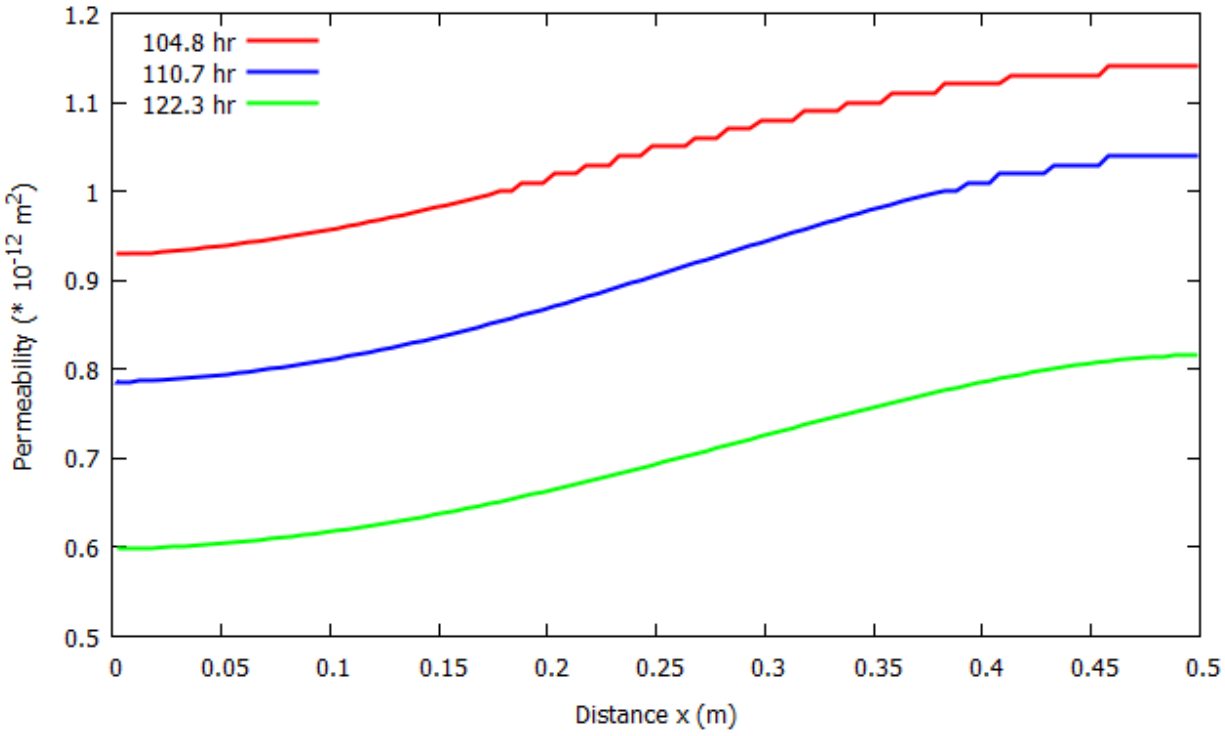

Fig. 5.5 (a): The permeability as a function of distance at several times for 2-phase injection scheme, for 0.5m column

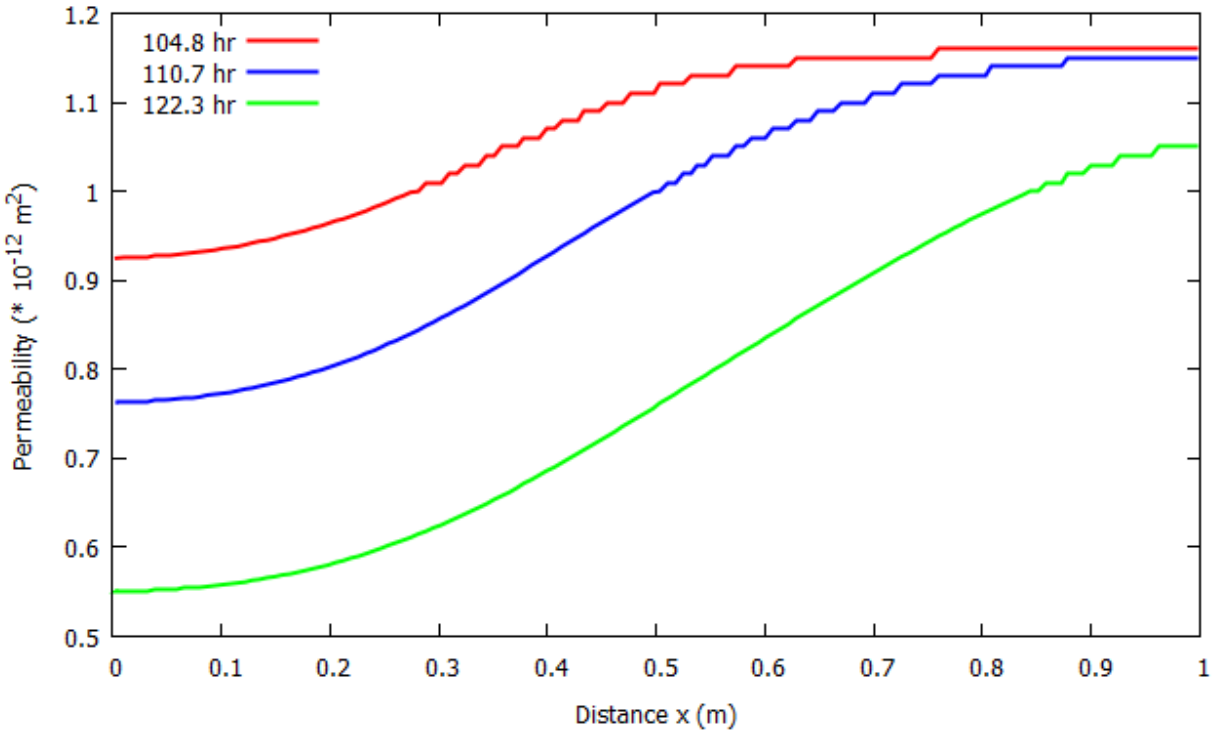

Fig. 5.5 (b): The permeability as a function of distance at several times for 2-phase injection scheme, for 1m column

Fig. 5.4 and Fig 5.5 show the porosity and permeability distribution along the column length after the treatment for 0.5m and 1m column, respectively. From Fig. 5.3(a), 5.4 (a) and 5.5(a), it is seen that for 0.5m column, at $x = 0$, for a precipitation of 597 $kg / m^3\ CaCO_3$, the porosity has decreased from 0.4 to 0.342, and the permeability has decreased from $1.157 \times 10^{-12}\ m^2$ to $5.99 \times 10^{-13}\ m^2$. Similarly, from Fig. 5.3(b), 5.4(b) and 5.5(b), it is seen that for 1m column at $x = 0$, for a precipitation of 721 $kg / m^3\ CaCO_3$, the porosity has decreased from 0.4 to 0.335, and the permeability has decreased from $1.157 \times 10^{-12}\ m^2$ to $5.51 \times 10^{-13}\ m^2$.

From Fig. 5.3(b), 5.4(b) and 5.5(b), it is seen that for 1m column the precipitation and change in porosity and permeability is relatively less at the end of the column, compared to 0.5m column.

5.3 1-Phase Scheme

5.3.1Results for Calcium Carbonate, Porosity and Permeability

Figure 5.6 shows the total amount of calcium carbonate in the domain for 0.5m and 1m column respectively.

For 0.5m column, after 2.8 hours, injection of Ca^{2+} is stopped. So from Fig. 5.6(a), the curve corresponding to 2.8 hour is the amount of calcite precipitated during Ca^{2+} injection period. Between 2.8 hours and 26.1 hours, calcite precipitation increases throughout the domain as a result of Ca^{2+} propagation and kinetic reaction taking place throughout the domain.

For 1m column, after 5.6 hours, injection of Ca^{2+} is stopped. So from Fig. 5.6(b), the curve corresponding to 5.6 hour is the amount of calcite precipitated during Ca^{2+} injection period. Between 5.6 hours and 29.1 hours, calcite precipitation increases throughout the domain as a result of Ca^{2+} propagation and kinetic reaction taking place throughout the domain.

Fig. 5.7 and Fig 5.8 show the porosity and permeability distribution along the column length after the treatment for 0.5m and 1m column, respectively, respectively. From Fig. 5.6(a), 5.7(a) and 5.8(a), it is seen that for 0.5m column, at $x = 0$, for a precipitation of 383 $kg/m^3\ CaCO_3$,

the porosity has decreased from 0.4 to 0.358, and the permeability has decreased from $1.157\times10^{-12}\ m^2$ to $7.25\times10^{-13}\ m^2$. Similarly, from Fig. 5.6(b), 5.7(b) and 5.8(b), it is seen that for 1m column at $x=0$, for a precipitation of 510 $kg/m^3\ CaCO_3$, the porosity has decreased from 0.4 to 0.351, and the permeability has decreased from $1.157\times10^{-12}\ m^2$ to $6.70\times10^{-13}\ m^2$.

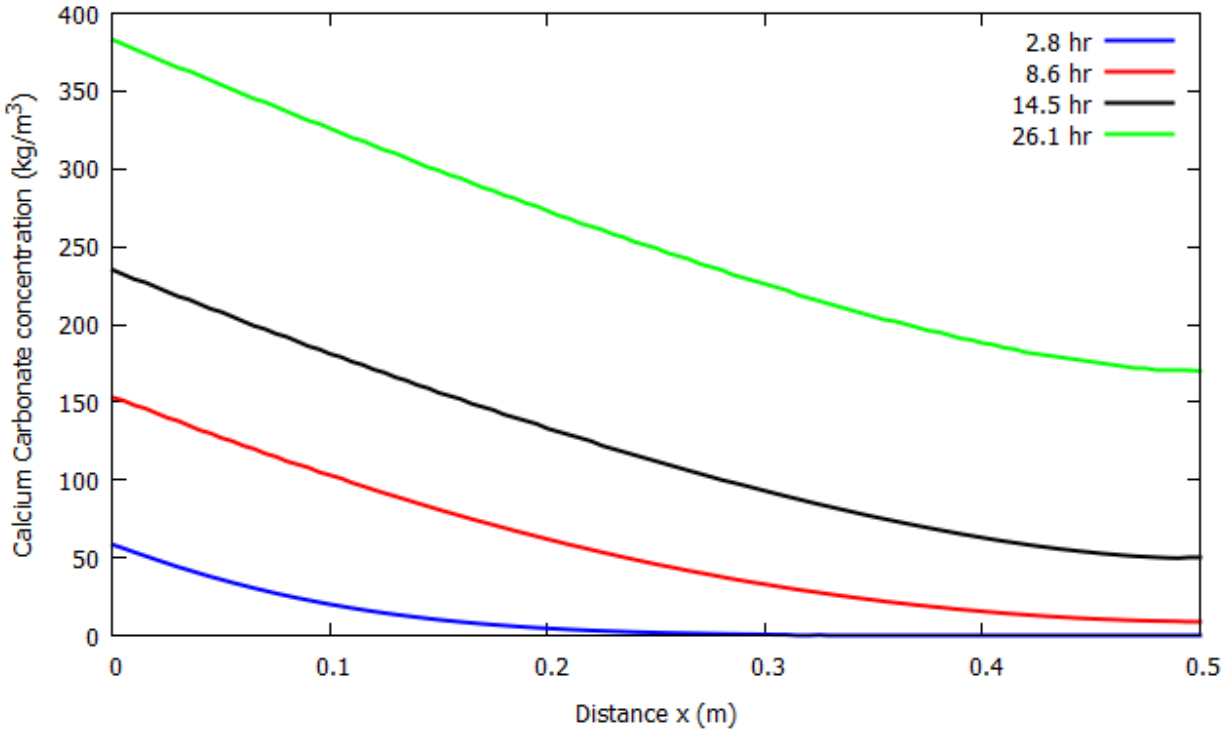

Fig. 5.6 (a): The concentration of calcium carbonate as a function of distance at several times for 1-phase injection scheme, for 0.5m column

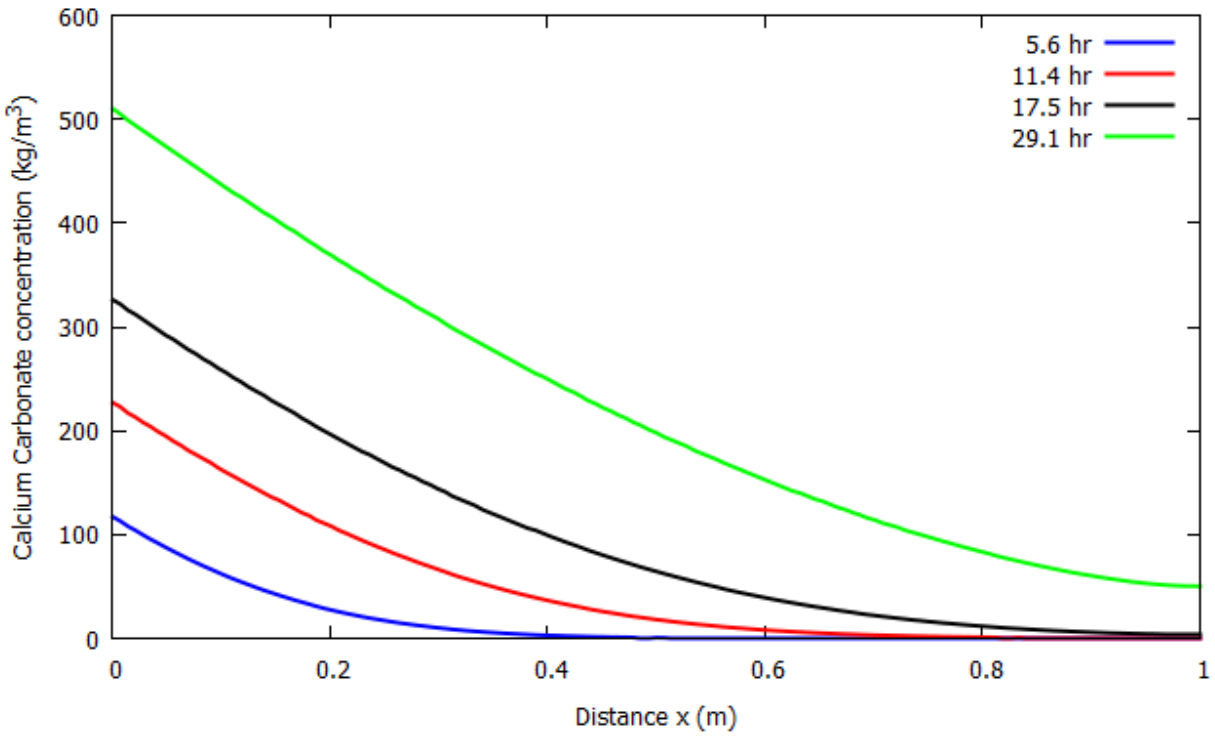

Fig. 5.6 (b): The concentration of calcium carbonate as a function of distance at several times for 1-phase injection scheme, for 1m column

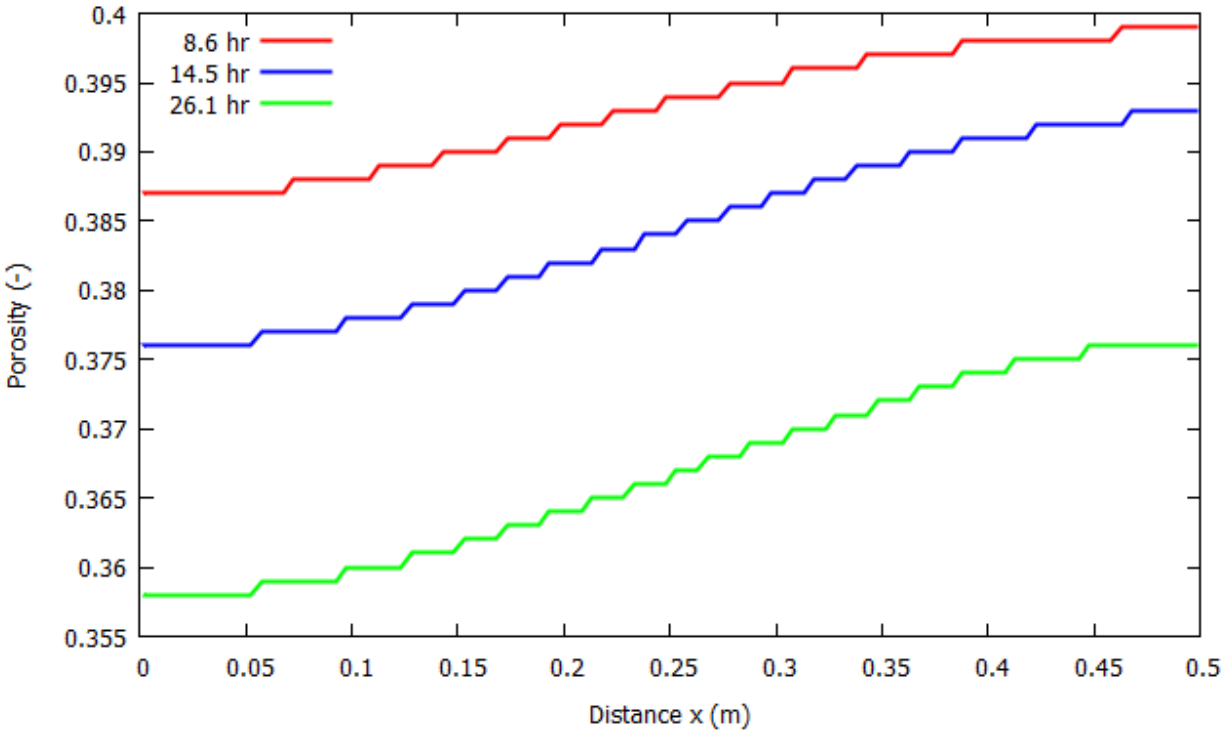

Fig. 5.7 (a): The porosity as a function of distance at several times for 1-phase injection scheme, for 0.5m column

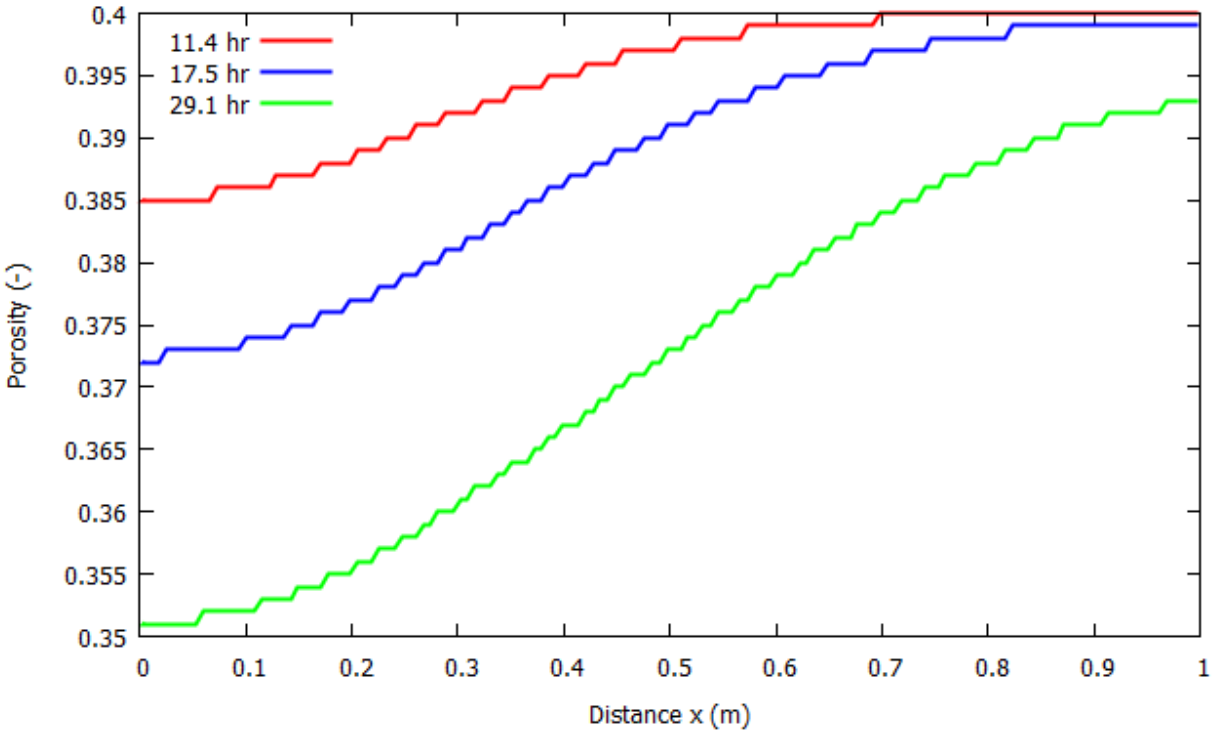

Fig. 5.7 (b): The porosity as a function of distance at several times for 1-phase injection scheme, for 1m column

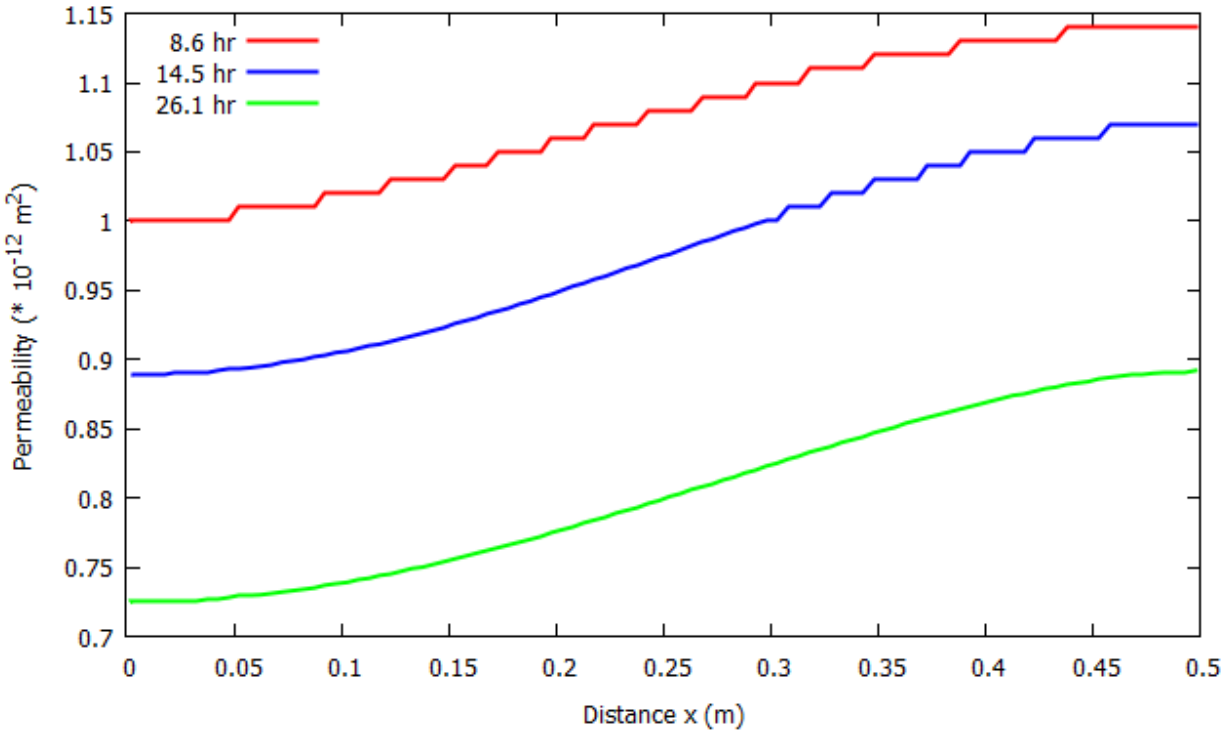

Fig. 5.8 (a): The permeability as a function of distance at several times for 1-phase injection scheme, for 0.5m column

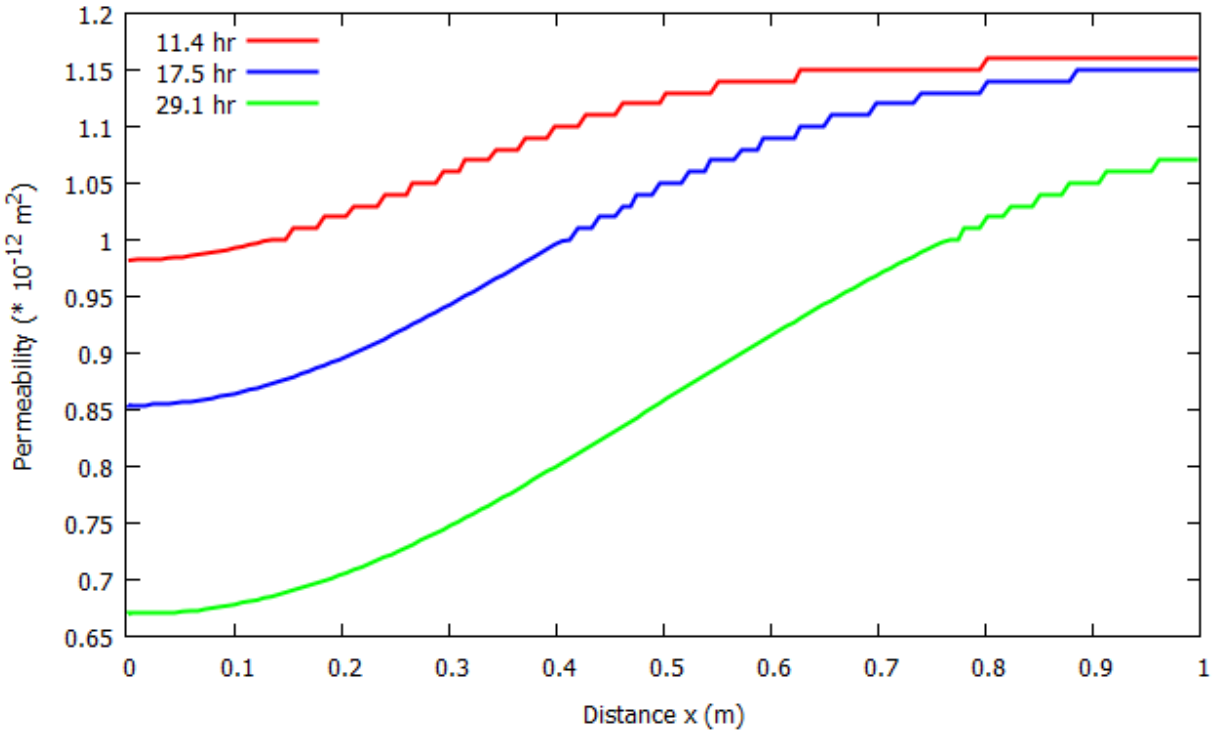

Fig. 5.8 (b): The permeability as a function of distance at several times for 1-phase injection scheme, for 1m column

From Fig. 5.6(b), 5.7(b) and 5.8(b), it is seen that for 1m column the precipitation and change in porosity and permeability is relatively less at the end of the column, compared to 0.5m column.

5.4 Comparison of mechanism between 2-Phase and 1-Phase Scheme

5.4.1 Comparison of mechanism for 0.5m column

From Fig. 5.9, for 0.5m column, it is seen that, for 2-phase scheme the amount of calcium carbonate precipitated is more than that of 1-phase scheme. For 2-phase scheme the amount of precipitated $CaCO_3$ at $x = 0$ is $597\, kg/m^3$, whereas for 1phase scheme the amount is $383\, kg/m^3$.

The reason behind this can be explained by the fact that in 2-phase scheme, a seating time is allowed so that urea and bacteria can propagate throughout the entire column and a homogeneous accumulation of carbonate ion is obtained throughout the column. When Ca^{2+} is supplied, only precipitation reaction takes place, as urea hydrolysis has already been completed. Due to this, $CaCO_3$ quickly precipitates. For 1-phase scheme, both urea and calcium chloride are supplied at the same time. But $CaCO_3$ cannot precipitate until urea hydrolysis takes place. So the precipitation rate is less. Also some Ca^{2+} gets washed away unreacted.

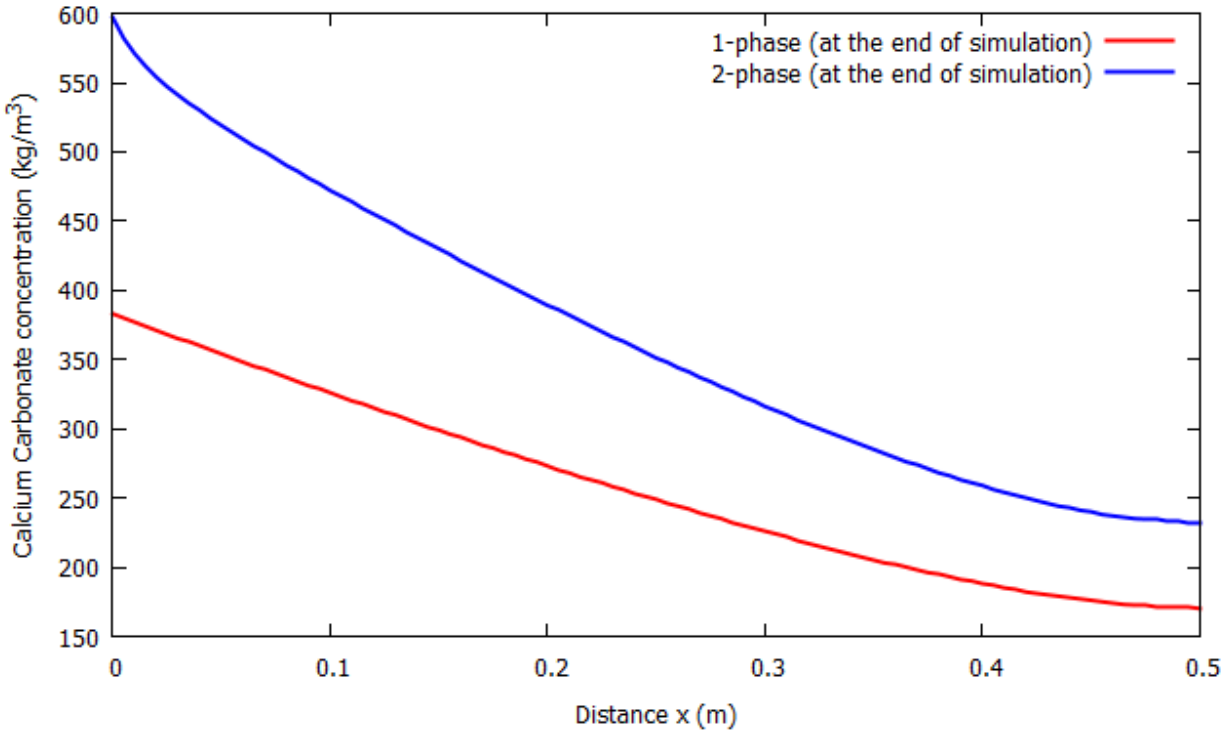

Fig. 5.9: Calcium Carbonate concentration along the column for 1-phase and 2-phase injection scheme for 0.5m column

Fig. 5.10 shows the porosity distribution throughout the column. At the end of both the simulations, for 2-phase simulation at $x = 0$, the porosity has decreased from 0.4 to 0.342, but for 1-phase scheme, it has decreased from 0.4 to 0.358. For 1-phase mechanism at the beginning there will be a lag between urea hydrolysis and calcite precipitation. Ca^{2+} cannot take part in the reaction until urea hydrolysis is done. So, at the beginning some unreacted Ca^{2+} gets flushed away from the column. But in 2-phase mechanism, there is no lag period, hence there is no unreacted Ca^{2+}.

Fig. 5.11 shows the permeability distribution throughout the column. At the end of both the simulations, for 2-phase simulation at $x = 0$, the permeability has decreased from $1.157 \times 10^{-12}\ m^2$ to $5.99 \times 10^{-13}\ m^2$, but for 1-phase scheme, it has decreased from $1.157 \times 10^{-12}\ m^2$ to $7.25 \times 10^{-13}\ m^2$. The reason is same as above.

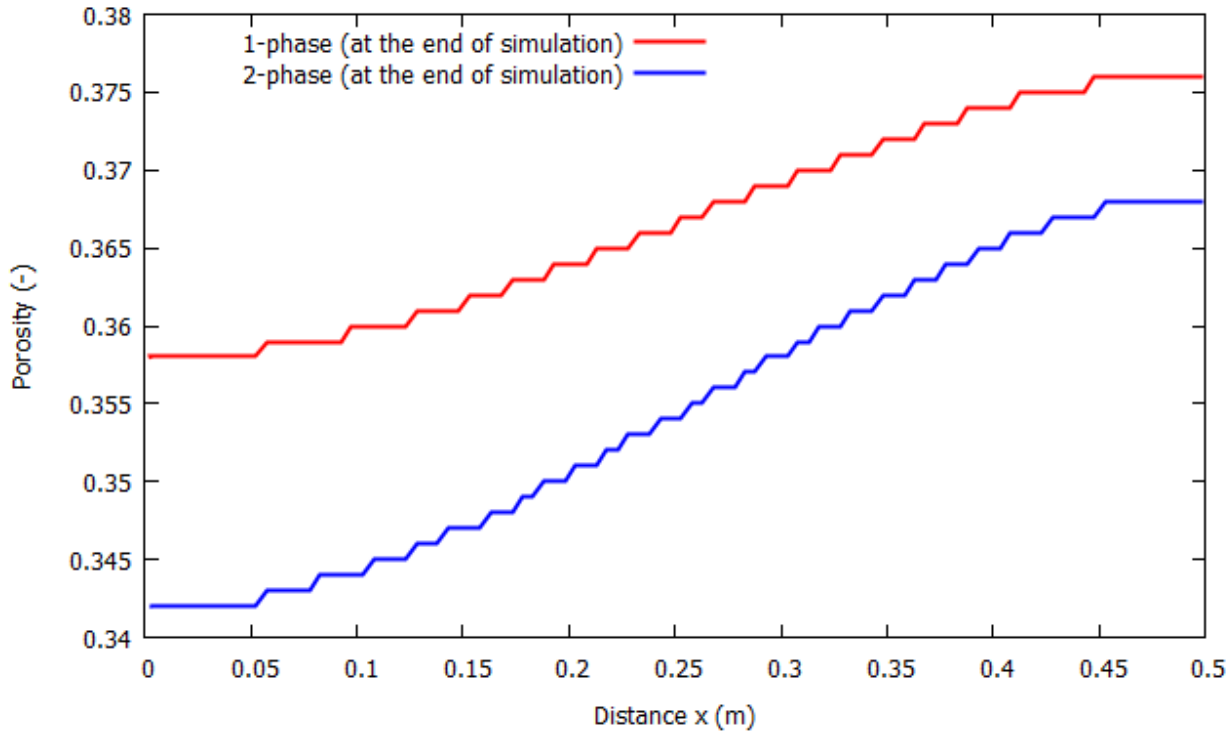

Fig. 5.10: Porosity distribution along the length of column for 1-phase and 2-phase injection scheme for 0.5m column

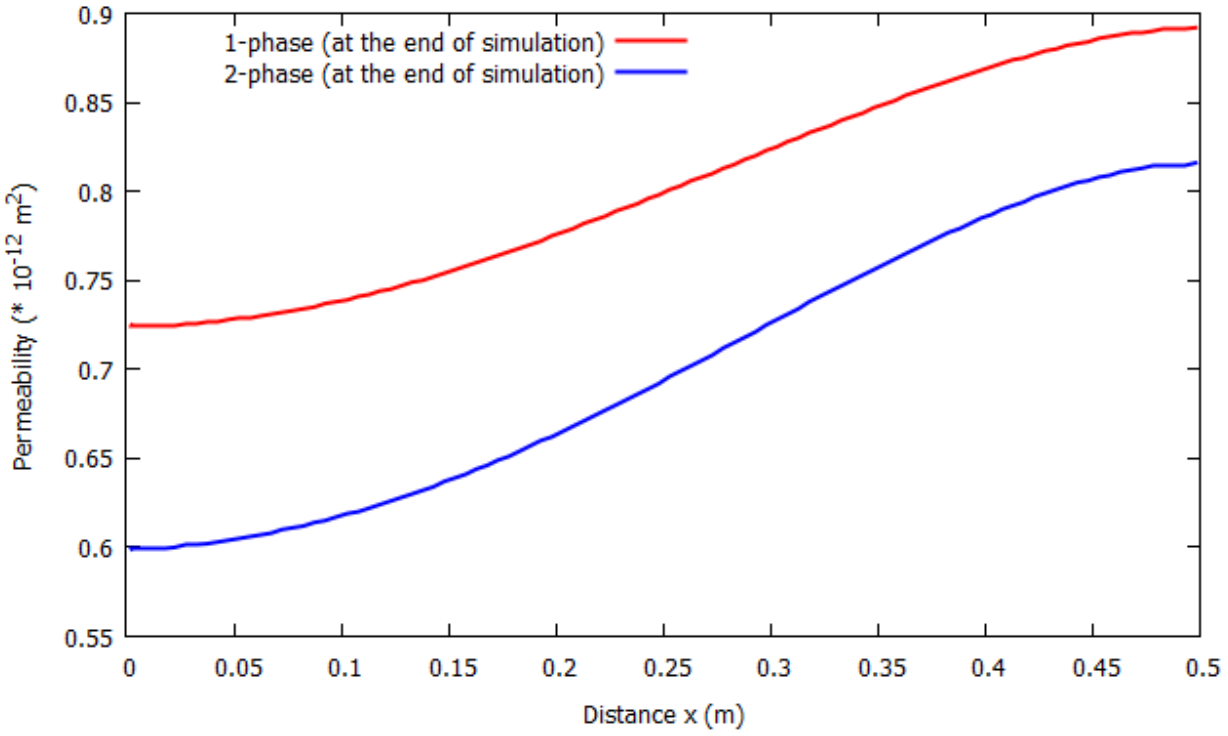

Fig. 5.11: Permeability distribution along the length of column for 1-phase and 2-phase injection scheme for 0.5m column

5.4.2 Comparison of mechanism for 1m column

From Fig 5.12, for 1m column, it is seen that, for 2-phase scheme the amount of calcium carbonate precipitated is more than that of 1-phase scheme. For 2-phase scheme the amount of

precipitated $CaCO_3$ at $x = 0$ is 721 kg / m^3, whereas for 1-phase scheme the amount is 510 kg / m^3. The reason behind this can be explained by the fact that in 2-phase scheme, a seating time is allowed so that urea and bacteria can propagate throughout the entire column and a homogeneous accumulation of carbonate ion is obtained throughout the column. When Ca^{2+} is supplied, only precipitation reaction takes place, as urea hydrolysis has already been completed. Due to this $CaCO_3$ quickly precipitates. For 1-phase scheme, both urea and calcium chloride are supplied at the same time. But $CaCO_3$ cannot precipitate until urea hydrolysis takes place. So the precipitation rate is less. Also some Ca^{2+} gets washed away unreacted.

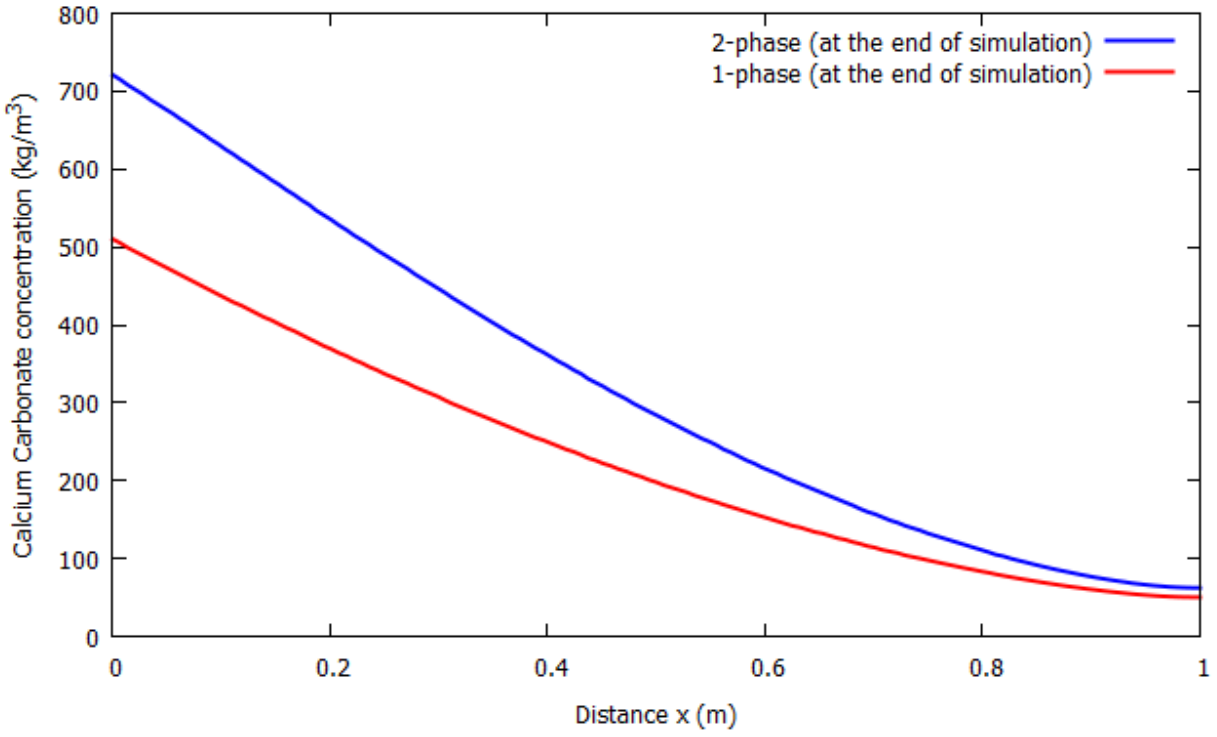

Fig. 5.12: Calcium Carbonate concentration along the column for 1-phase and 2-phase injection scheme for 1m column

Fig. 5.13 shows the porosity distribution throughout the column. At the end of both the simulations, for 2-phase simulation at $x = 0$, the porosity has decreased from 0.4 to 0.335, but for 1-phase scheme, it has decreased from 0.4 to 0.351. For 1-phase mechanism at the beginning there will be a lag between urea hydrolysis and calcite precipitation. Ca^{2+} cannot take part in the reaction until urea hydrolysis is done. So, at the beginning some unreacted Ca^{2+} gets flushed away from the column. But in 2-phase mechanism, there is no lag period, hence there is no unreacted Ca^{2+}.

Fig. 5.14 shows the permeability distribution throughout the column. At the end of both the simulations, for 2-phase simulation at $x = 0$, the permeability has decreased from $1.157 \times 10^{-12}\, m^2$ to $5.51 \times 10^{-13}\, m^2$, but for 1-phase scheme, it has decreased from $1.157 \times 10^{-12}\, m^2$ to $6.70 \times 10^{-13}\, m^2$. The reason is same as above.

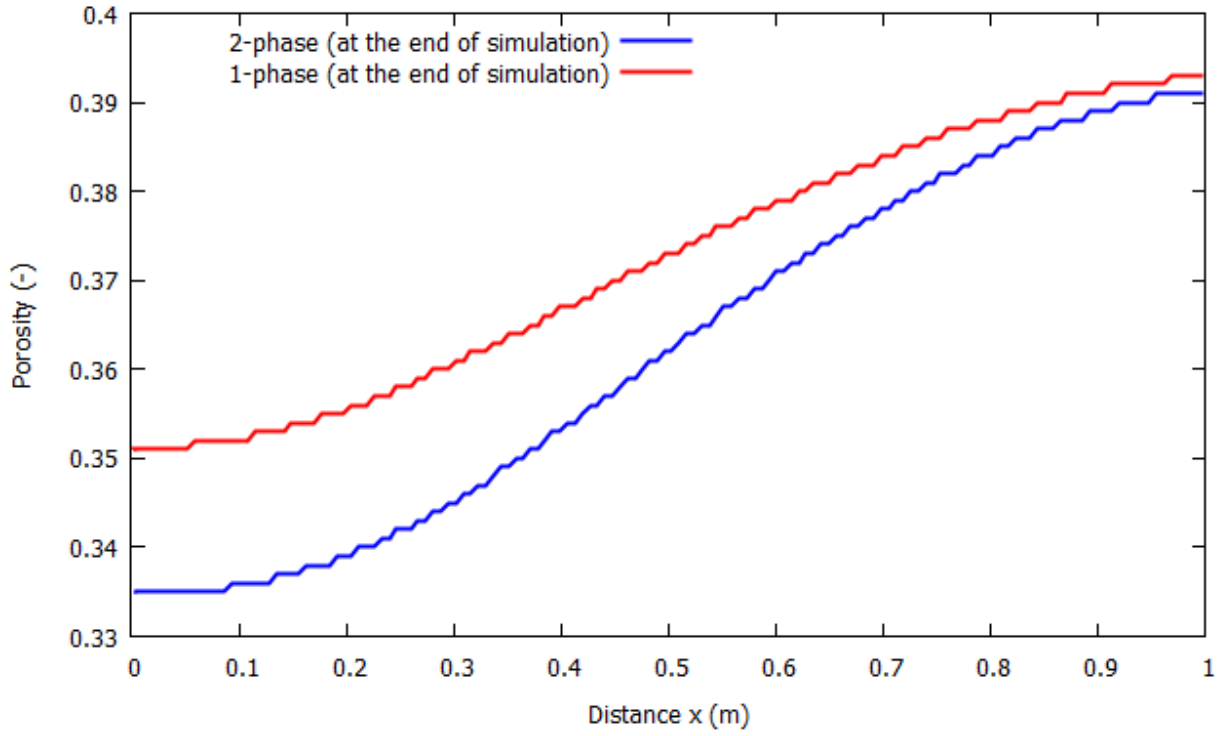

Fig. 5.13: Porosity distribution along the length of column for 1-phase and 2-phase injection scheme for 1m column

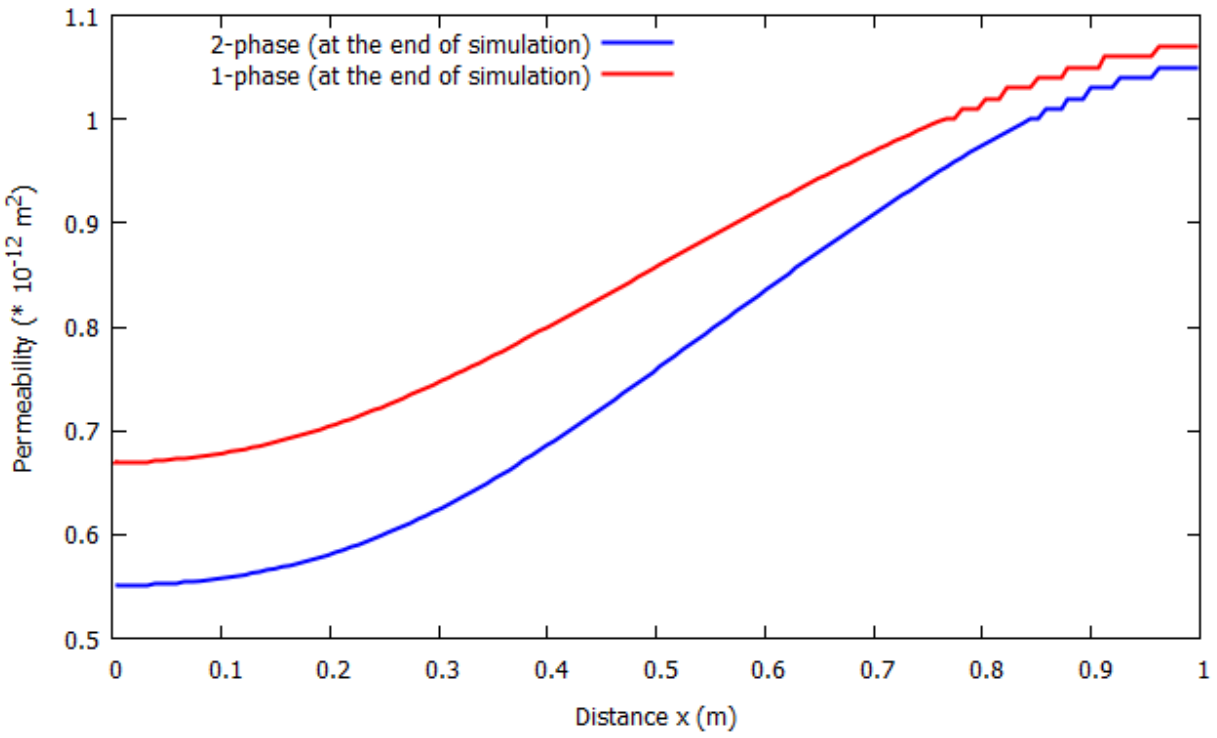

Fig. 5.14: Permeability distribution along the length of column for 1-phase and 2-phase injection scheme for 1m column

Chapter 6

Summary and Future Extensions

6.1 Summary

A model has been formulated to describe the Biogrout process. The model gives insight into several aspects of the Biogrout process. The Biogrout process influences several properties of the subsoil. The precipitation of the solid calcium carbonate decreases the porosity and the permeability. According to the model, for 0.5m column, a precipitation of 597 $kg/m^3\ CaCO_3$ has decreased the porosity from 0.4 to 0.342, and the permeability from $1.157\times10^{-12}\ m^2$ to $5.99\times10^{-13}\ m^2$. For 1m column, a precipitation of 721 $kg/m^3\ CaCO_3$ has decreased the porosity from 0.4 to 0.335, and the permeability from $1.157\times10^{-12}\ m^2$ to $5.51\times10^{-13}\ m^2$.

It is also found that for 1m column the precipitation and change in porosity and permeability is relatively less at the end of the column, compared to 0.5m column.

For 1-phase mechanism at the beginning there will be a lag between urea hydrolysis and calcite precipitation. Ca^{2+} cannot take part in the reaction until urea hydrolysis is done. So, at the beginning some unreacted Ca^{2+} gets flushed away from the column. But in 2-phase mechanism, there is no lag period, hence there is no unreacted Ca^{2+}. Hence 2-phase mechanism gives more calcite precipitation.

In the first part of the column, more calcium carbonate precipitated than in the end of the column. The reason is that many component molecules did already react in the first part of the column and could not reach the end of the column within the simulation time. Significant amount of precipitation has been observed over the entire length of the column for both 2-phase and 1-phase mechanism and for both small and larger domain.

The model has been created under several assumptions. These assumptions should be validated using experiments. The first assumption was that the process is governed by the biochemical reaction (2.1). However, in reality this reaction happens in several steps. Some of these steps are equilibrium reactions that depend on the pH. Other assumptions are that the retardation factors are equal to 1 and that the total volume of the fluid does not change due to the hydrolysis of urea and the precipitation of calcium carbonate. These assumptions should be verified (van Wijngaarden et al., 2011).

It has also been assumed that calcium carbonate precipitates locally and will not be transported. Calcium carbonate can precipitate in several ways. It can attach to sand grains but can also form

crystals. When these crystals are large enough, they will stick in the pore throats and it can be assumed that they are not transported. However, when these crystals are small, probably they can be transported. It should be verified if this phenomenon is really negligible (van Wijngaarden et al., 2011).

Another assumption is that the distribution of bacteria is homogeneous and decay of bacteria with time is neglected. These bacteria have been placed in the subsurface by injecting a solution with bacteria and a fixation fluid. The bacteria are assumed to attach to the solid particles and this effect will be enlarged by the fixation fluid. This fixation fluid causes the flocculation of bacteria and hence they cannot easily flow out anymore but will be filtered by the sand. It is not likely that these processes will result in a homogeneous bacteria distribution (van Wijngaarden et al., 2011). The formula for the reaction rate includes the constants k_{urea} *and* k_{precip} .Experiments should be done to determine the value of these constants. Further research should be done to find out which circumstances influence the reaction rate and a better formula for the reaction rate should be found.

To calculate the intrinsic permeability the Kozeny–Carman relation has been used. This empirical relation turns out to be a good relation for many cases. It is questionable if this is also true for the Biogrout process, with its changing porosity. In this study, any relation can be incorporated, but since this issue is not crucial here, the use of the classical Kozeny–Carman relation is maintained (van Wijngaarden et al., 2011).

The assumption that the fluid density and viscosity is constant and not dependent on the various concentrations, is also a simplification of reality. As a result of precipitation, the produced solid phase components get detached from the fluid and become a part of the solid matrix. This could lead to a decrease in density and viscosity.
Hence, although the assumptions should be verified, the model is a good tool to get insight into the process.

For engineering design, it is necessary to know the relation between the calcium carbonate and the mechanical characteristics of the soil. For the strength of the soil, it is important where the calcium carbonate precipitates. Calcium carbonate, connecting sand grains, will give a contribution to strength, while loose crystals hardly will. Furthermore, calcium carbonate isa polymorph, which means that several mineral types exist with similar molecular composition(amorphous calcium carbonate, vaterite and calcite). The crystal properties (size, shapeand mineral type) are dependent on, among others; the precipitation conditions (Van Paassen2009) and will result in a different contribution to strength (van Wijngaarden et al., 2011).

With this method, loose sands are stabilized to a desired strength varying from loosely cemented sand to moderately strong rock (unconfined compressive strengths of 0.2–20 MPa) (Whiffin et al., 2007; Harkes et al., 2009). The corresponding amount of precipitated calcium carbonate varies from 30 to 600 kg / m^3 of soil. Once precipitated, the calcium carbonate will only dissolve very slowly, either when continuously flushed by acidic groundwater or as a result of acidifying processes in the pores (e.g. degradation of biomass). When sufficient calcium carbonate is

precipitated, durable soil stabilization can be achieved. At present, the principle has been applied successfully on a scale of 1 m^3 and the first tests on demonstration scale (100 m^3) have been executed (van Paassen et al., 2009, 2010).

6.2 Future Extension

- Decay of bacteria and sorption effect of reaction components can be considered to make the model more accurate.
- Density dependent flow analysis has to be performed.
- Experimental determination of the kinetic rates.
- Experimental validation of the proposed model.

References

1. Al Qabany A, Mortensen B, Martinez B, Soga K, DeJong J. Microbial carbonate precipitation: correlation of S-wave velocity with calcite precipitation. In: Han J, Alzamora DA, editors. Advances on geotechnical engineering. Proceedings of geo-frontiers, March 13–16, 2011. Dallas, Texas, USA: Geotechnical Special Publications; 2011
2. Barkouki TH, Martinez BC, Mortensen BM, Weathers TS, De Jong JD, Ginn TR, Spycher NF, Smith RW, Fujita Y (2011) Forward and Inverse Bio-Geochemical Modeling of Microbially Induced Calcite Precipitation in Half-Meter Column Experiments. Transp Porous Med (2011) 90:23–39
3. DeJong JT, Fritzges MB, Nüsslein K. Microbially induced cementation to control sand response to undrained shear. J Geotech Geoenviron Eng 2006;132(11):1381–92
4. Fan, C.-C. & Su, C.-F. 2008. "Role of roots in the shear strength of rootreinforced soils with high moisture content." Ecological Engineering 33(2): 157-166
5. Ferris F. G. and Stehmeier L. G. (1992) Bacteriogenic mineral plugging. Patent 5,143,155. Washington D.C.: U.S. Patent Office.
6. Ferris F. G., Phoenix V., Fujita Y., Smith R. W. (2003) Kinetics of calcite precipitation induced by ureolytic bacteria at 10 to 20°C in artificial groundwater, Geochimica et Cosmochimica Acta, 67(8), 1701-1722.
7. Ferris F. G., Stehmeier L.G., Kantzas A., Mourits F. M. (1996) Bacteriogenic mineral plugging, Journal of Canadian Petroleum Technology, 13, 57-67.

8. Fujita Y., Ferris F. G., Lawson R. D., Colwell F. S., Smith R. W. (2000) Calcium carbonate precipitation by ureolytic subsurface bacteria, Geomicrobiology Journal, 17, 305-318.
9. Hammes F., Seka A., de Knijf S., Verstraete W. (2003a) A novel approach to calcium removal from calcium-rich industrial wastewater, Water Research, 37, 699-704.
10. Harkes, M.P., Booster, J.L., van Paassen, L.A., van Loosdrecht, M.C.M., Whiffin, V.S., 2008. Microbial induced carbonate precipitation as ground improvement method—bacterial fixation and empirical correlation CaCO3 vs. strength. International conference on BioGeoCivil Engineering, Delft
11. Ivanov, V. & Chu, J. 2008. "Applications of microorganisms to geotechnical engineering for bioclogging and biocementation of soil in situ." Reviews in Environmental Science and Biotechnology 7(2): 139-153.
12. Kolditz O, Bauer S, Bilke L, Bottcher N, Delfs JO, Fischer T, Gorke UJ, Kalbacher T, Kosakowski G, McDermott CI, Park CH, Radu F, Rink K, Shao H, Shao HB, Sun F, Sun YY, Singh AK, Taron J, Walther M, Wang W, Watanabe N, Wu Y, Xie M, Xu W, Zehner B (2012) OpenGeoSys: an open-source initiative for numerical simulation of thermo-hydro-mechanical/chemical (THM/C) processes in porous media
13. Laloui L, Fauriel S (2011) BIOGROUT PROPAGATION IN SOILS. Multiscale and Multiphysics Processes in Geomechanics, SSGG, pp. 77–80.
14. Li L, Qian CX, Zhao YH, Zhu YT (2013) Enzyme kinetic characterization of microbe-produced urease for microbe-driven calcite mineralization. Reac Kinet Mech Cat (2013) 108:51–57

15. Martinez BC, DeJong JT, Ginn TR (2014) Bio-geochemical reactive transport modeling of microbial induced calcite precipitation to predict the treatment of sand in one-dimensional flow. Computers and Geotechnics 58 (2014) 1–13
16. Mitchell A. C. and Ferris F. G. (2005) The coprecipitation of Sr into calcite precipitates induced by bacterial ureolysis in artificial groundwater: Temperature and kinetic dependence, Geochimica et Cosmochimica Acta, 69(17), 4199-4210.
17. Mitchell, J. K., and Santamarina, J. C. (2005). "Biological considerations in geotechnical engineering." J. Geotech. Geoenviron. Eng., 10.1061, 1222–1233
18. Palandri, J.L., Kharaka, Y.K., 2004. A compilation of rate parameters of water–mineral interaction kinetics for application to geochemical modeling. Open File Report 2004-1068, U.S. Geological Survey, Menlo Park, California.
19. Parks SL (2009) Kinetics of calcite precipitation by ureolytic bacteria under aerobic and anaerobic conditions. MS Thesis submitted to Montana State University, Department of Chemical and Biological Engineering.
20. Ramachandran S. K., Ramakrishnan V., Bang S. S. (2001) Remediation of concrete using microorganisms, ACI Materials Journal, 98(1), 3-9.
21. Rebata-Landa V. Bio-Mediated Geochemical Effects. PhD thesis, Georgia Institute of Technology; 2007.
22. Riley R. G. and Zachara J. M. (1992) Chemical contaminants on DOE lands and selection of contaminant mixtures for subsurface science research, DOE/ER-0547T, U.S. Department of Energy, Office of Energy Research, Washington, D.C.
23. Stocks-Fischer S., Galinat J. K., Bang S. S. (1999) Microbiological precipitation of CaCO3, Soil Biology and Biochemistry, 31, 1563-1571.

24. van Paassen LA, Daza CM, Staal M, Sorokin DY, van der Zon W, van Loosdrecht MCM (2010). Potential soil reinforcement by biological denitrification, Ecological Engineering 36 (2010) 168–175.
25. van Paassen LA. Biogrout: ground improvement by microbially induced carbonate precipitation. PhD thesis, TU Delft; 2009.
26. van Wijngaarden WK, Vermolen FJ, van Meurs GAM, Vuik C (2011). Modellingbiogrout: a new ground improvement method based on microbial-inducedcarbonate precipitation. Transp Porous Media 2011;87(2):397–420.
27. van Wijngaargen WK, Vermolen FJ, van Meurs GAM, Vuik C (2010) Modelling the new Soil Improvement Method Biogrout: Extension to 3D. Numerical Mathematics and Advanced Applications 2009 2010, pp 893-900
28. van Wijngaargen WK, Vermolen FJ, van Meurs GAM, Vuik C (2013) A robust method to tackle pressure boundary conditions in porous media flow: application to biogrout. Comput Geosci (2014) 18:103–115
29. Veizer J. (1990) Trace elements and isotopes in sedimentary carbonates, in Reeder R. J. (ed.) Carbonate: mineralogy and chemistry, Reviews in Mineralogy, 11, Chelsea, MI: Mineralogical Society of America, 265-300.
30. Warren L. A., Maurice P. A., Parmar N., Ferris F. G. (2001) Microbially mediated calcium carbonate precipitation: Implications for interpreting calcite precipitation and for solid-phase capture of inorganic contaminants, Geomicrobiology Journal, 18(1), 93-115.
31. Whiffin V. A, van Paassen L. A, Harkes M. P. (2007) Microbial carbonate precipitation as a soil improvement technique, Geomicrobiology Journal, 24(5), 417-423.

32. Whiffin VS. Microbial CaCO3 precipitation for the production of biocement PhD thesis, School of Biological Sciences and Biotechnology, Perth, Murdoch University; 2004.